UNIVERSITATEA NATIONALA DE STIINTA SI TEHNOLOGIE

POLITEHNICA BUCURESTI

DOCTORAL SCHOOL OF ELECTRICAL ENGINEERING

THESIS

CONTRIBUTIONS REGARDING THE POSSIBILITY OF REUSE OF BATTERIES IN ELECTRICAL SUPPLY OF DATA CENTERS

SUMMARY

Eng. GKANATSIOS STAVROS

PhD supervisor: Univ. Prof. emeritus Ph.D. Eng. Costin CEPISCĂ

Keywords: Power Supply, Data Center, UPS, Batteries, Modeling

Thankings

Special thanks to Prof. Univ. emeritus Ph.D. Eng. Costin Cepișca for the continuous, high-quality scientific guidance that helped me complete the research with this doctoral thesis.
I would like to thank the professors of the Department of Measurements, electrical devices and static converters of the Faculty of Electrical Engineering of the POLITEHNICA University in Bucharest, for the support given in the completion of the doctoral thesis, especially Professor Dr. Eng. George Călin Serițan and Mr. Ph.D. Eng. Bogdan Enache.
Special thanks to my family for their constant support, encouragement and understanding.

Author

Contents Thesis

Introduction

The sharp development of battery production for electric vehicles leads, in the near future, to the appearance of a significant amount of batteries that are replaceable but can still be used in some electrical energy storage applications that do not require operation at rapid charge/discharge shocks .
Among the possible reuse solutions, I stopped at the use of batteries in the emergency power supply of Data Centers. Current UPSs use classic Lead-acid batteries, but with the appearance of Li-Ion batteries replaced in electric vehicles, an important battery market appears that requires technical possibilities to test the capabilities of use within the energy structures of Data Centers or in other electricity storage situations.
The objective of the research carried out in this doctoral thesis is to create extended models for batteries that can be used in the structure of UPSs in Data Centers, of the Pb-acid, Li-Ion, Li-Ion second life type, models that are used in the design and realization of a system for determining the state of health of the batteries equipping a UPS.
Chapter 1 of the doctoral thesis presents the current development of Data Centers, constructive solutions, infrastructures and technical achievements.
Chapter 2 refers to technical solutions for powering Data Centers and how to assess energy efficiency.
Chapter 3 analyzes the UPS system and battery usage, indicating system structure, battery fabrication technologies, testing, modeling, and performance management methods.
Chapter 4 contains the model made for a UPS system with the Matlab Simulink/Simscape software package. A time domain analysis was chosen, starting from the mathematical equations of each component of the UPS system. This model allows the analysis of the operation and the determination of the dynamic characteristics under different conditions of use.
Chapter 5 presents research results on extending the battery bank model to incorporate different realization technologies. Own solutions developed for the characterization of battery parameters and the assembly embedded in the UPS structure demonstrate that there are viable solutions for replacing lead-acid batteries that equip UPSs in Data Centers with Li-Ion second life batteries.
Chapter 6 contains research on determining the optimal time to replace batteries taking into account their state of health. The first step in the design of a dedicated device was to analyze the methods of determining the age of the battery, with the choice of the method of the two discharge pulses. Practically, hardware and software, an intelligent device that allows the determination of the state of charge and the health of the battery was realized, the experimental results highlighting the applicability of the method used. This device can be attached to the UPS in a Data Center or other electrical energy storage structure to provide battery management regardless of battery type

CHAPTER 1. The current situation of the technical development of Data Centers

1.1. Data centers (DC) – definitions and standards

The data center is defined by the ANSI/TIA-942 standard as:

"A building or part of a building whose primary function is to house a computer room and related support areas" [1].

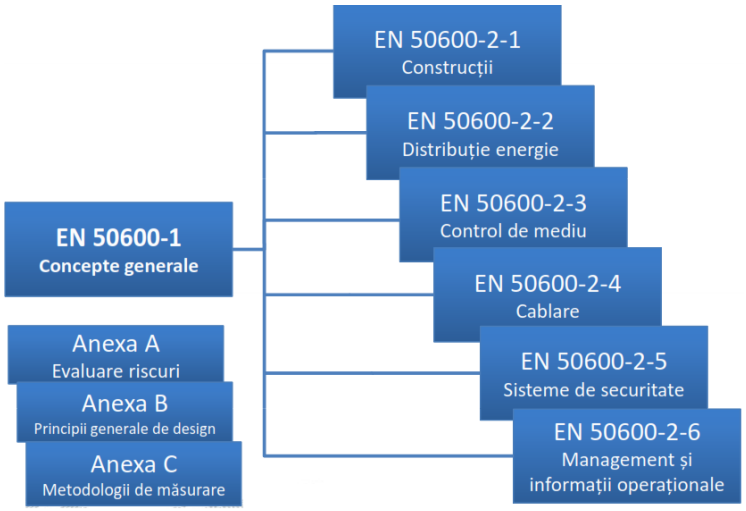

Fig. 1.1. Standard EN 50600 [3]

The EN 50600 standard brings clarifications for operators and beneficiaries of Data Centers, through clear specifications regarding the planning, construction and operation of Data Center infrastructures – Fig.1.1.

1.2. Architectures and constructive solutions for Data Centers

A Data Center always contains [10]:

- a place to locate servers, switches and storage equipment;
- equipment necessary to ensure the appropriate environmental conditions for optimal functioning of IT equipment;
- ways to connect to servers for internal and external clients;
- energy supply solution in conditions of capacity and time period appropriate for IT equipment to function continuously.

The ANSI/TIA-942 standard establishes 4 levels of reliability and resilience (Tier) of Data Center implementation based on ensuring a desired operational reliability between 99.671% functional availability (maximum 28.8 hours/year power outages) and 99.995% (maximum 0.4 hours/year power interruption). The choice of a certain level (Tier) for the realization of the Data Center leads to the dimensioning of the implementation structure and the number of redundant equipment. Table 1 shows the main requirements and comparisons between tiers (Tier).

Table 1. Performance standards by level (Tier)

Tier Requirement	Tier 1	Tier 2	Tier 3	Tier 4
Source	System	System	System	System + System
Redundancy of system components	N	N+1	N+1	Minimum N+1
Distribution paths	1	1	1 normal 1 alternative	2 active simultaneously
Compartmentalization	No	No	No	Yes
With concurrent maintenance	No	No	Yes	Yes
Fault tolerance (single event)	No	No	No	Yes

1.3. National and International Data Centers

A situation of the evolution of investments in the field of data centers worldwide is presented in the following figure, supporting the development trends.

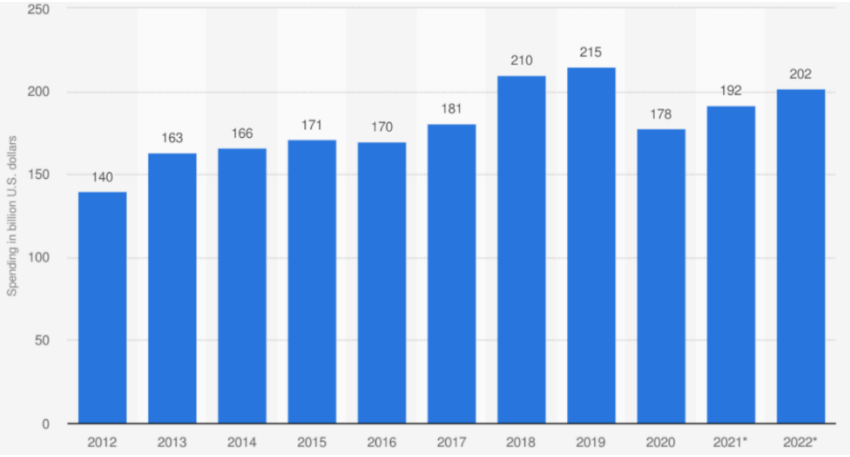

Fig. 1.9. Global Data Center Investments (2012-2022). Source: www.statista.com

At the level of 2021, 2594 Data Centers of various sizes from 295 distributors were operational, most in the countries indicated in the following figure.

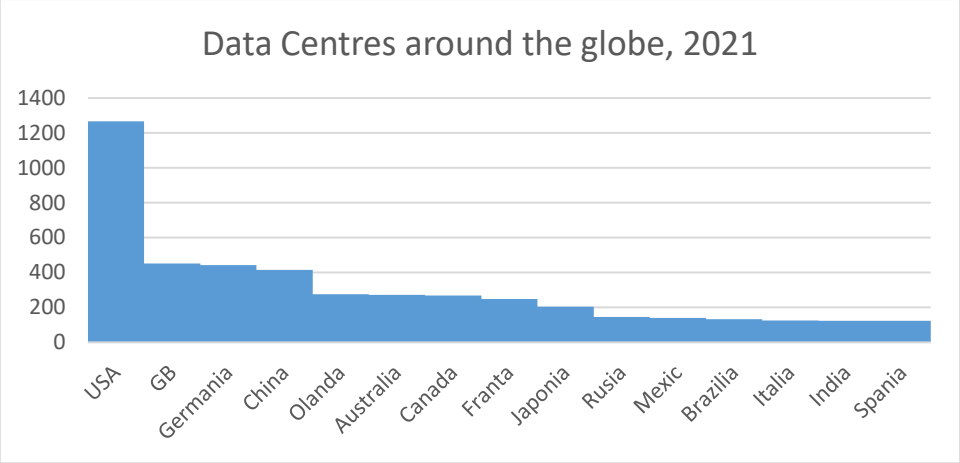

Fig. 1.10. Data Centers around the globe. Source: www.statista.com

1.4. Infrastructure of a Data Center

The functional architecture of a Data Center [19], includes, in addition to the computing and communications infrastructure (servers, specific software, data archiving, data staging genome, data presentation, real-time monitoring, capacity management) and other equipment that ensures its functionality.

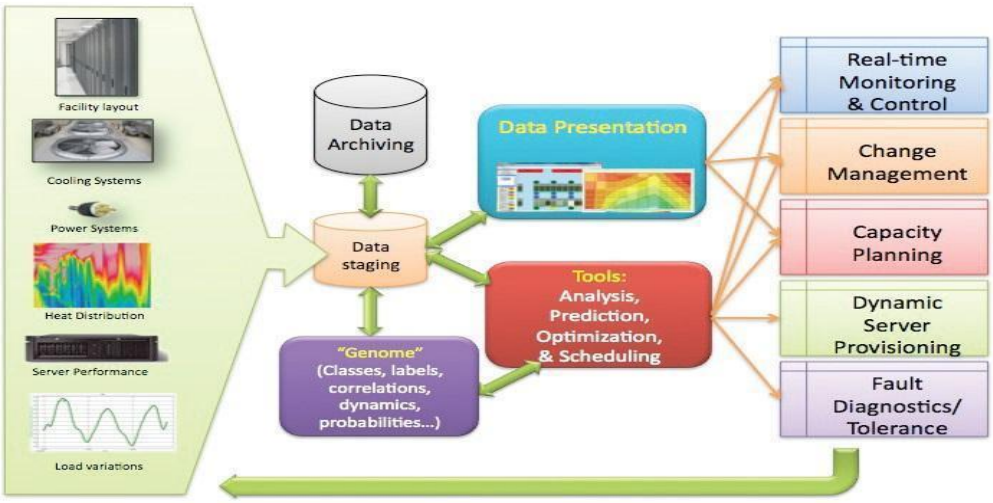

Fig. 1.18. Data Center Architecture [20].

It can be seen that the physical infrastructure in the Data Center is represented by: power supply, electrical distribution, precision air conditioning, racks, fire extinguishing, access control, monitoring of environmental conditions and infrastructure management. [20]

The power supply system: a brief presentation is shown in Fig.1.20 [21].

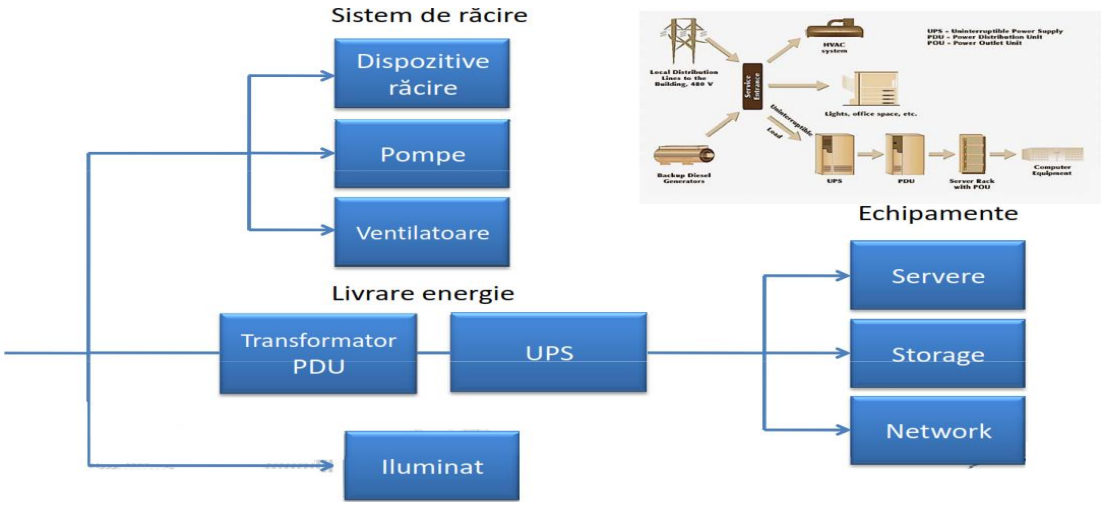

Fig. 1.20. Electricity supply system structure for Data Center [22].

CHAPTER 2. Solutions for the power supply of the Data Center

2.1. Topologies and standards

Fig.2.1 shows the typical distribution of energy consumption at a Data Center.

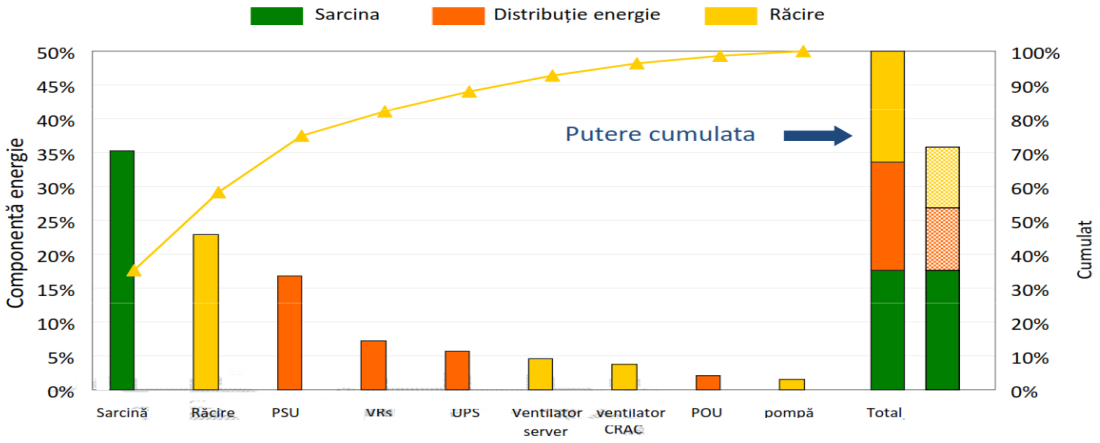

Fig. 2.1. Energy consumption at a Data Center (source: Intel.com)

In the thesis, different variants of electrical network configurations in small and medium-sized Data Centers are illustrated.

There are standardized (ANSI/BICSI 002-2011) 5 classes related to the reliability levels of the electrical infrastructure of Data Centers.

ANSI/BICSI 002-2011, Clase

Clasa	Descriere (evaluare dpdv al sistemului electric)
F0	Centrul de date cu **un singur traseu** de distribuție, **fără:** sursa de putere alternativă, UPS, împământare IT corespunzătoare
F1	Centrul de date cu **un singur traseu** de distribuție
F2	Centrul de date cu un singur traseu de distribuție, cu **componente reduntante**
F3	Centrul de date care poate fi **întreținut și operabil concomitent**
F4	Centrul de date **tolerant la defecțiuni**

2.2. Example of powering a Tier 3 Data Center with inclusion solar energy generation equipment

A proprietary electrical power supply scheme for a smaller Tier 3 Data Center, mounted in a container, is presented, the configuration including a power supply from photovoltaic sources.

2.3. Assessing the energy efficiency of the Data Center

Energy efficiency is a method of evaluating and tracking electricity consumption in a Data Center. It is used as an indicator:

PUE=(Total energy consumed from the network)/(Energy consumed by installed IT equipment) (2.1)

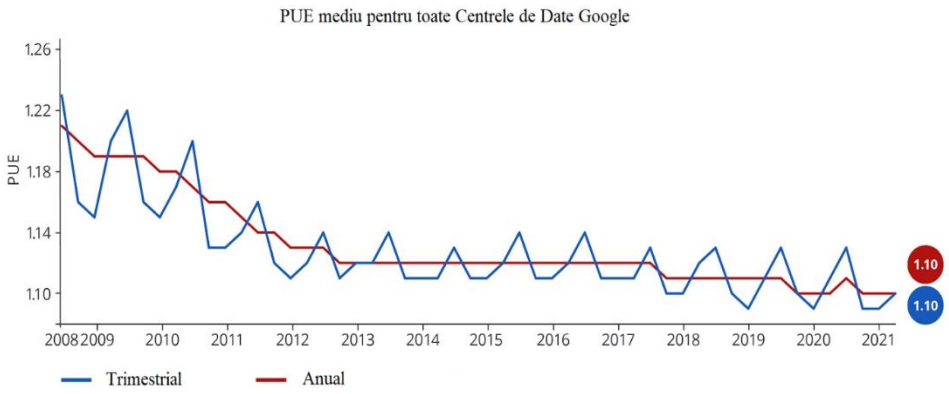

Fig. 2.10. Google Data Center- Average PUE

Chapter 3. UPS System and Battery usage

3.1. Structure of a UPS system

The solution of the uninterruptible power supply UPS (Uninterruptible Power Supplies) + battery has good results from the perspective of cost and reliability, being preferable in the realization of a Data Center. [28], [29].

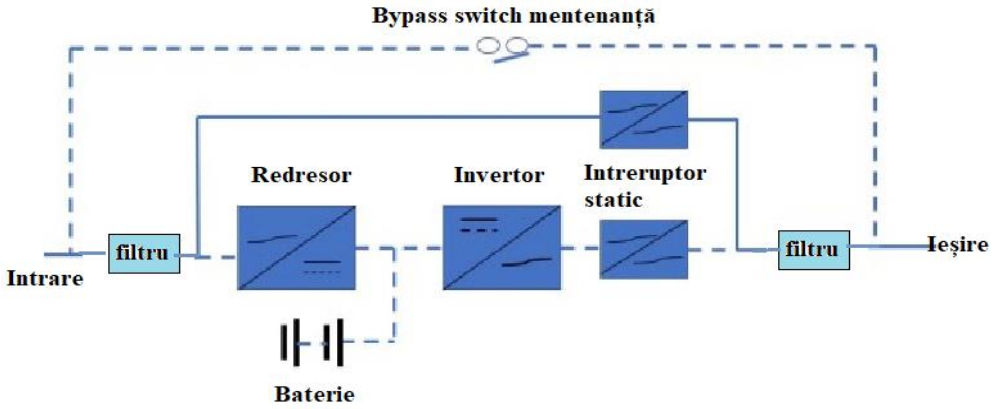

Fig. 3.1. UPS system components [31]

The thesis presents different solutions for UPS+ battery solutions in specific schemes for different classes of Data Centers. [31], [32].

3.2. Electrochemical storage of electricity

Table 3.1. Main existing battery technologies [34]

Tehnology	Lead-acid	Ni-Cd	Li-ion
Cell voltage (V)	2	1.2	3～3.6
Wh/kg	25～35	40～50	100～600
Lifetime (cycles)	300	300～500	＞500
Field of use	Automobile IT, UPS, Energy storage	Railway Sector	Electric car, IT

3.2.1. Pb-acid batteries

In the current UPS+ battery systems VRLA batteries (Valve Regulated Lead Acid - Batteries with pressure regulating valve) are mainly used, manufactured and tested in accordance with the IEC SR EN 60896-21/22 standard, 2V cells, 6V and 12V blocks with capacities between 7 Ah and 3500 Ah.

3.2.2. Lithium-based batteries

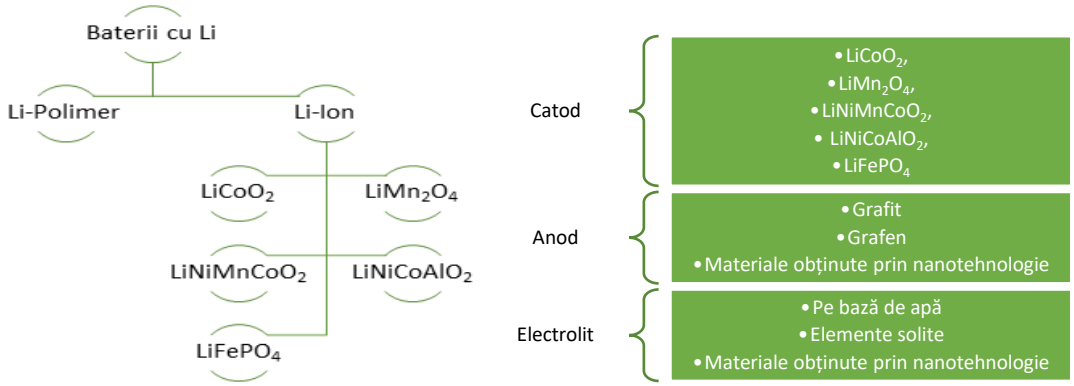

Fig. 3.9. Lithium-based batteries

3.3. Functional parameters of batteries

The functional parameters that must be taken into account in modeling and optimizing the correct operation of a battery are presented.

3.3. 1. State of charge

The state of charge (SoC) is defined as the ratio between the current capacity of a battery C(t) and its nominal capacity Cn:

$$SoC = \frac{C(t)}{C_n}$$

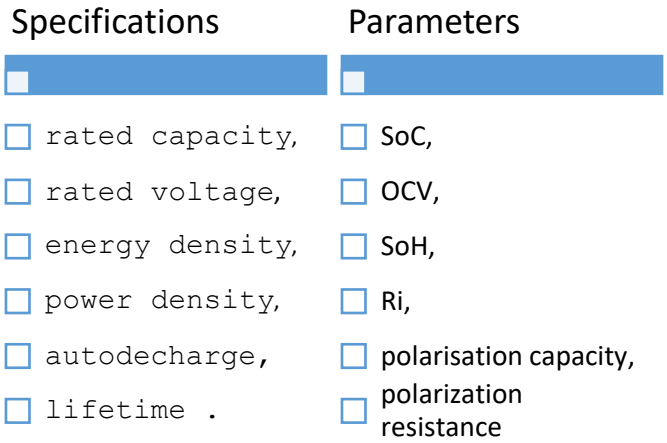

Fig. 3.11. Functional parameters of an electric battery

The nominal capacity Cn, represents the maximum load that can be stored in the battery. It is expressed in ampere-hours [Ah] and does not change during the life of the battery.
The current capacity of a battery is defined in the battery discharge operation. If the battery is considered to be fully charged at time t = 0 and the discharge current is i(t), the discharged electric charge is given by the relation (3.7):

$$C_d = \int_0^{t_d} i(t)dt$$

where td is the download time.
In these conditions:

$$SoC = 1 - \frac{\int_0^{t_d} i(t)dt}{C_n}$$

3.3.2. Open Circuit Voltage (OCV)

Open circuit voltage is the voltage across the terminals of a battery, at a given SoC and temperature, in the absence of any discharge or charge current.
For most types of batteries, the OCV voltage has a linear dependence on the SoC, according to the relationship:

$$OCV(t) = a_1 \cdot SoC(t) + a_0$$

where: SoC(t) is the instantaneous value of the state of charge of the battery; a0 is the voltage value for SoC = 0%; a1 voltage value for SoC = 100%.

3.3.3. Internal resistance

The most used method for measuring the internal resistance consists in determining the difference in the value of the voltage at the terminals, when applying a known discharge current I - Fig.3.14.

$$R_i = \frac{\Delta V}{I}$$

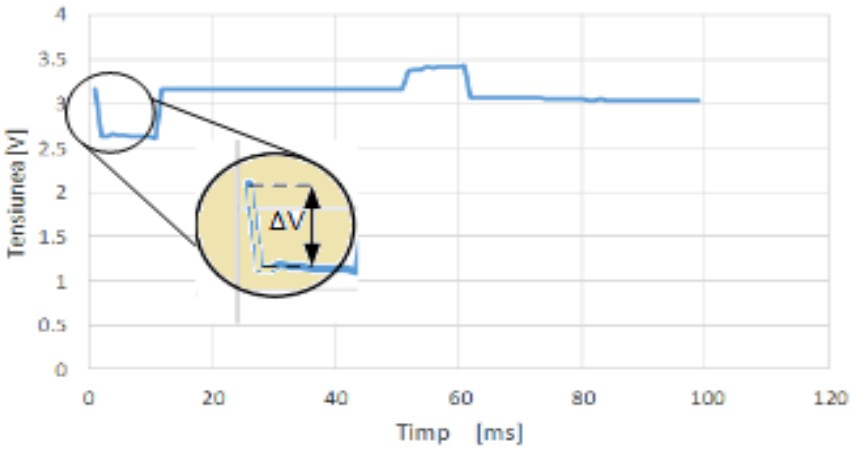

Fig. 3.14. Determination of internal resistance of LiFePO4 type battery

3.3.4. State of Health (SoH)

The state of health (SoH) indicates the battery's ability to supply/receive energy at a certain point in time, being defined in terms of capacity loss:

$$SoH = \frac{C_{ef}}{C_n}$$

3.4. Battery testing to determine parameters

Battery parameters are determined by the methods and procedures indicated in: "USABC Test Procedures Manual" [46] and "PNGV Test Manual" [47].

• basic tests: constant current discharge, peak power determination, constant power discharge, thermal performance, partial discharge;

• tests to determine the lifetime of a battery: accelerated aging, simulation of real situations, etc.

These tests are presented in detail in the thesis.

3.5. Modeling batteries

The battery model characterizes, in a software algorithm, the behavior of the battery in response to various external and internal conditions and can then be used to estimate the state of the battery at any time.

The most used modeling methods are electrochemical, analytical, those based on the analogy with electric circuits and the combined ones [48]. Fig.3.18 shows the most studied and recommended variants for each of these methods.

The thesis analyzes the modeling methodology followed for each type of model.

3.6. Battery Management Systems (BMS)

Management systems (BMS) for batteries of various construction types aim to ensure a check of key operational parameters during charging and discharging (voltages, currents, internal and ambient temperature of the battery) and to provide signals to protective devices in case any of the parameters would be outside normal limits. The structure and functions of the BMS depend on the application in which the particular battery is used.

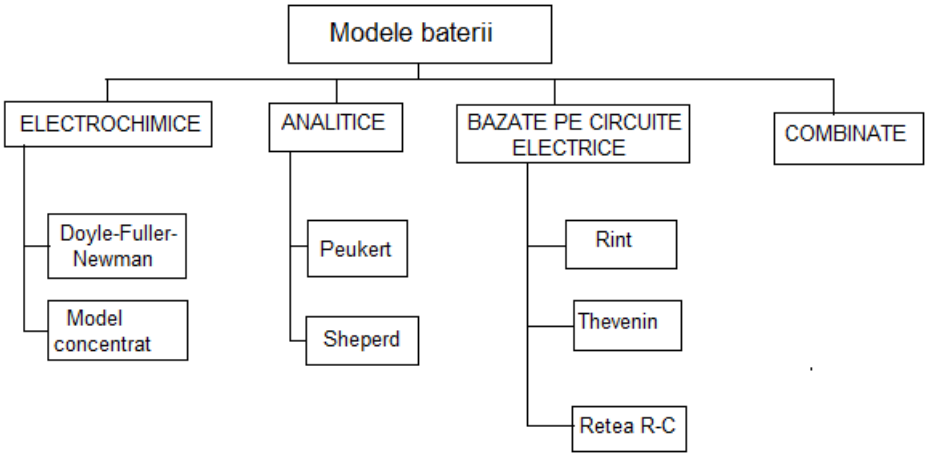

Fig. 3.18. Battery models

In order to extend the service life and operational safety it has gradually become a practice to implement balancing devices as part of the battery management system. The current methods used to balance batteries are as follows:

active methods

- energy is transferred between the component batteries

passive methods

- the energy of overcharged batteries is dissipated as heat.

The main balancing methods for batteries are presented in the thesis.

Chapter 4. Modeling a UPS system

I opted for a time domain analysis starting from the mathematical relationships that describe the operation of each component in the UPS system.
I used as input data for the model I made those obtained from an online UPS of the APC Smart-UPS 15000 VA model, which supplies a Data Center of a company with 50 employees.
The parameters of this system are [90]:
• Supply voltage – 230 V
• Working frequency – 50 Hz
• Debited electrical power - 1500 VA/ 900 W
• Efficiency – 92%
• Trigger time – 2 – 4 ms
• Battery – VRLA, APCRBC155, voltage 48V capacity 9 Ah, to which is added an external battery SRT48BP 48V, 18 Ah.
• Battery charging power – 108 W
The operating characteristic according to the manufacturer is shown in Fig. 4.1.

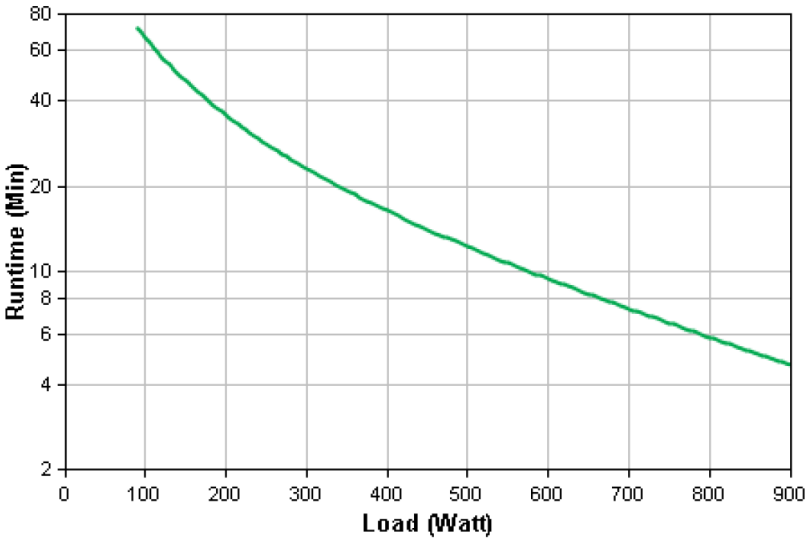

Fig.4.1. UPS discharge characteristic subject to modeling [90]

4.1. Block structure UPS

The block structure of the analyzed UPS system is based on the general operation scheme and is realized with the Matlab Simulink software package - Fig. 4.2.

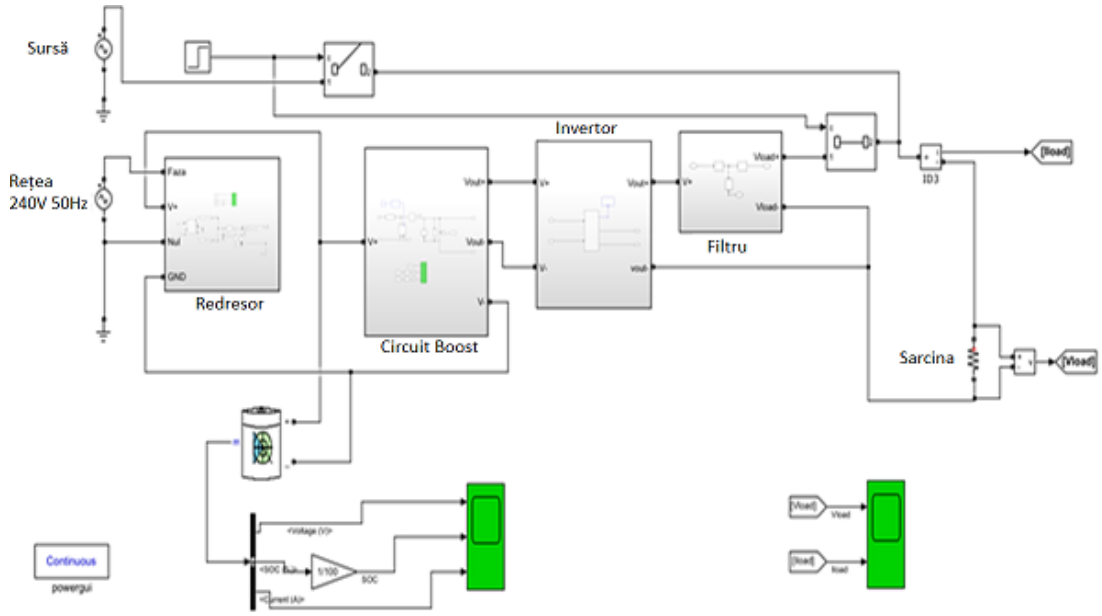

Fig. 4.2. The completed UPS model

The rectifier used in the UPS model is a mid-point bi-alternating rectifier with the following model – Fig. 4.4. The waveforms of other voltages and currents obtained from running the model are shown in Fig. 4.5.

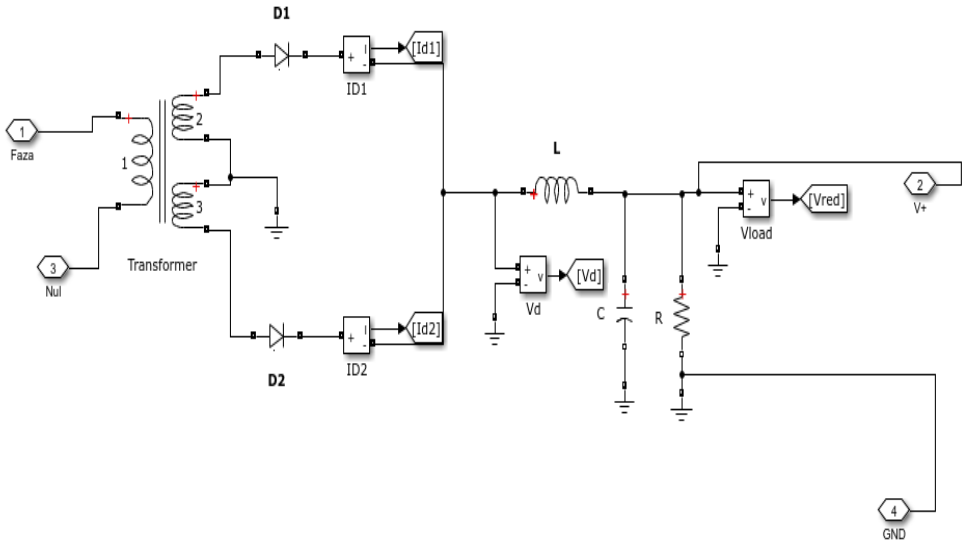

Fig. 4.4. Rectifier with midpoint implemented

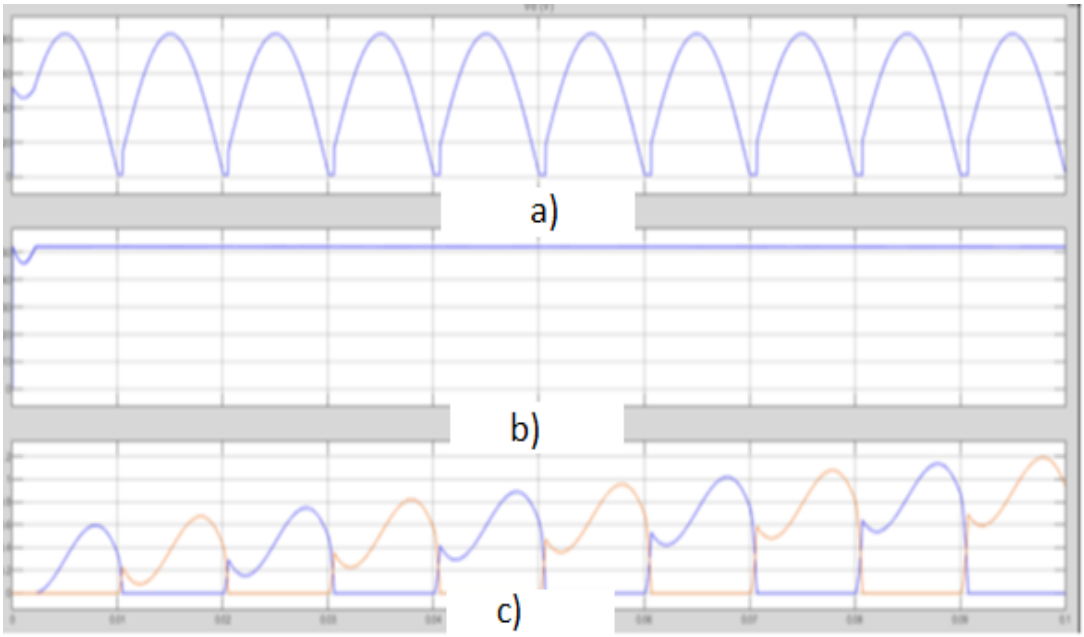

a) Rectified voltage waveform
b) Output capacitor output waveform
c) Waveforms of currents through diodes D1 and D2

Fig. 4.5. Operation of midpoint rectifier

The battery bank used in the UPS model consists of:
- 4 VRLA 12V Pb-acid batteries with a nominal capacity of 9 Ah connected in series.
- 1 external battery of 18 Ah composed of 8 VRLA batteries 2P4S configuration.

The battery bank model was made based on the generic Pb-acid battery model implemented in the Matlab program which has the operating equations [79]:
• when discharging:

$$U_{out} = E_0 - K \cdot \frac{Q}{Q -} \cdot i^{\square} - K \cdot \frac{Q}{Q -} \cdot_{\square} \left(\frac{exp(s)}{Sel(s)} \right)$$

• at charging

$$U_{out} = E_0 - K \cdot \frac{Q}{Q + \cdot i^{\square} - K \cdot \frac{Q}{Q -} \cdot_{\square} \left(\frac{exp(s)}{Sel(s)} \cdot \frac{1}{s} \right)}$$

All batteries were assumed to be identical and were of the VRLA 12V type with a capacity of 9Ah.

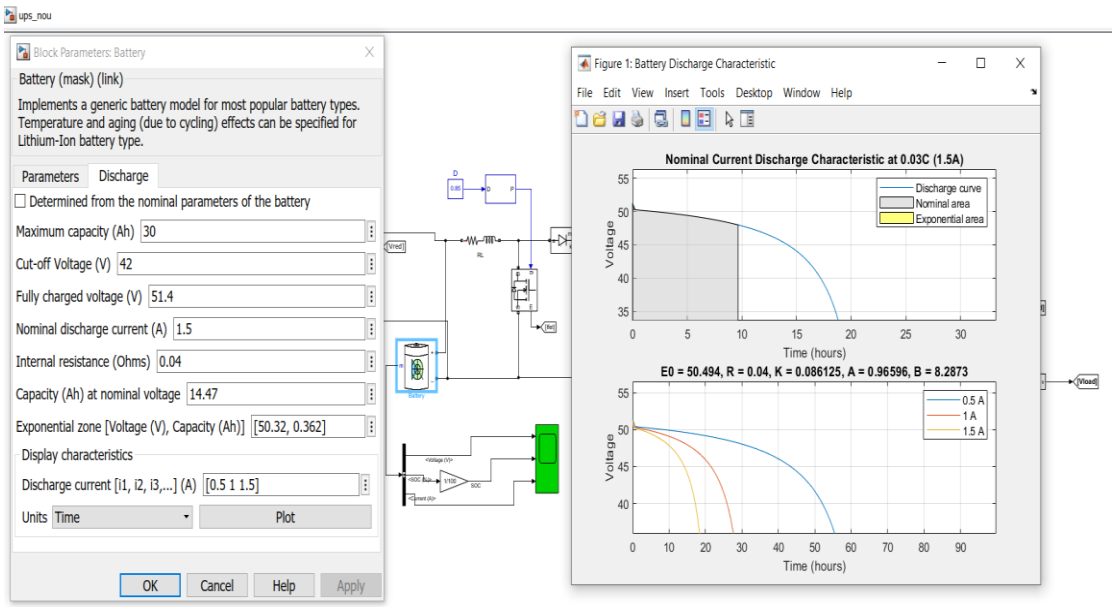

Fig. 4.7. Modeling of the Pb-acid battery bank Un = 48V, Q = 27 Ah

After running the battery model, the waveforms are shown in Fig. 4.8:

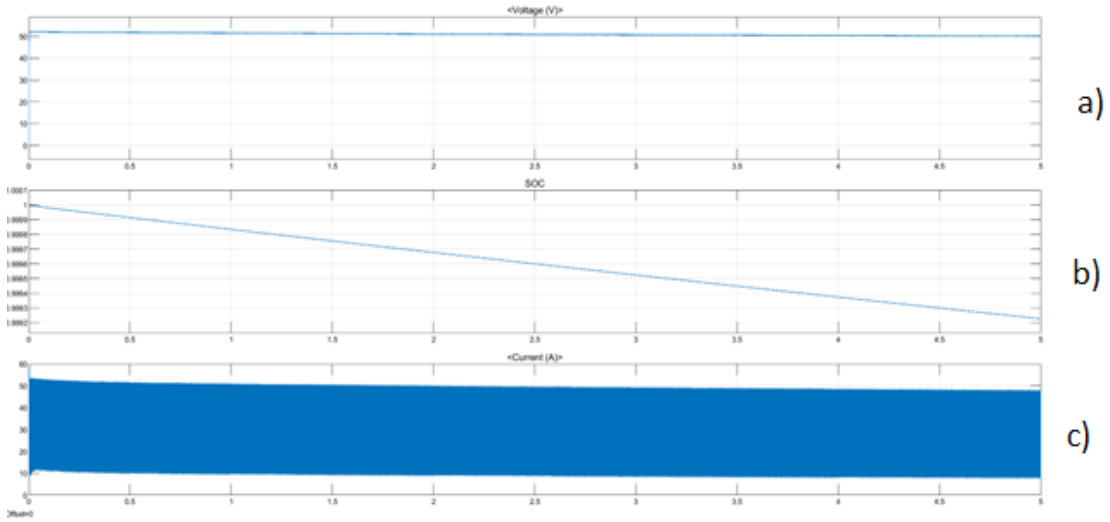

Fig. 4.8. Evolution of battery bank parameters when switching from online to offline UPS mode

4.4. Boost circuit

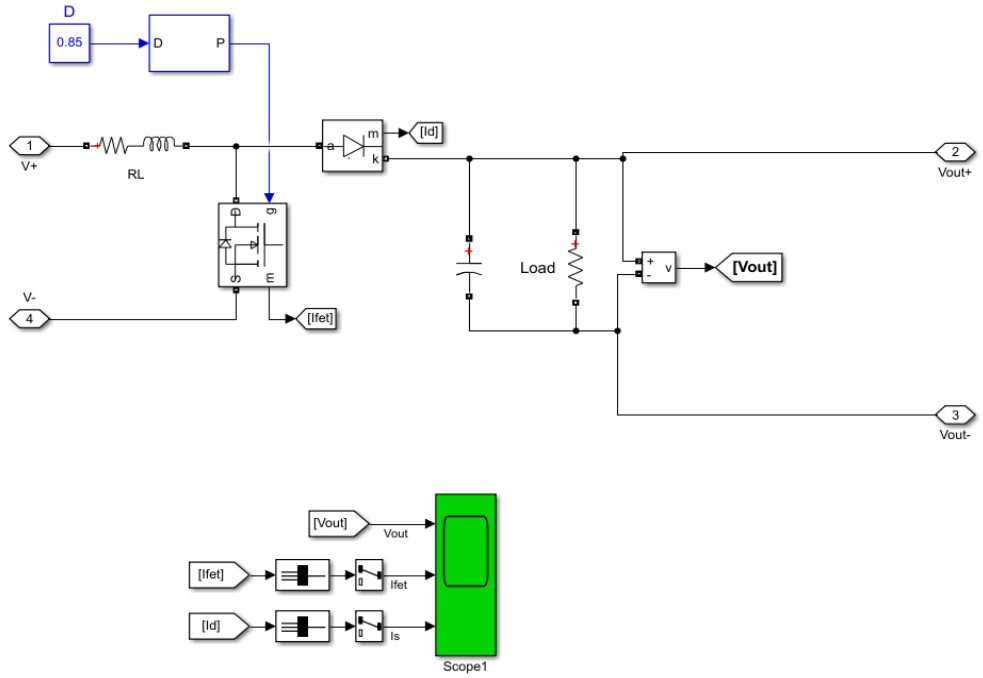

Fig. 4.10. Boost converter implemented

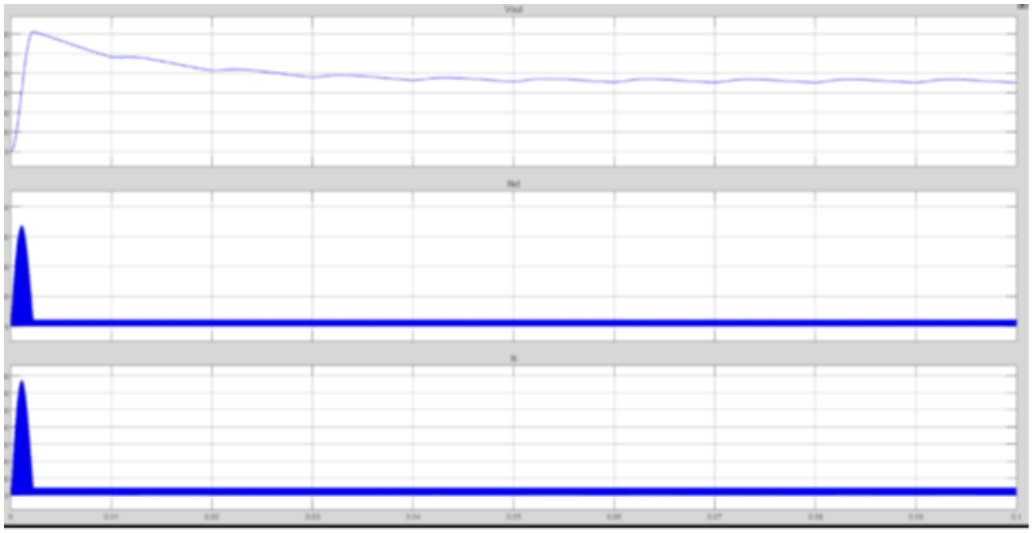

a) Output voltage
b) Current intensity through the MOSFET switch
c) The intensity of the currents through the diode

Fig. 4.11. Boost converter operation

4.5. Inverter

The structure from which the creation of this block started is shown in Fig. 4.12. The inverter is composed of 4 MOSFET type transistors that form the arms of a bridge and that are controlled to obtain an alternating output voltage with the frequency $f_o = \frac{1}{T_c}$ The modeling of this block was done using the Inverter block from the SimScape library with the default configuration – Fig. 4.13.

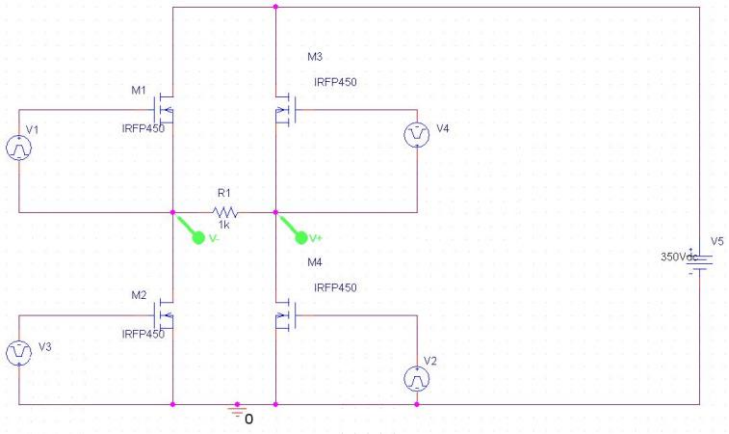

Fig. 4.12. Single-phase inverter

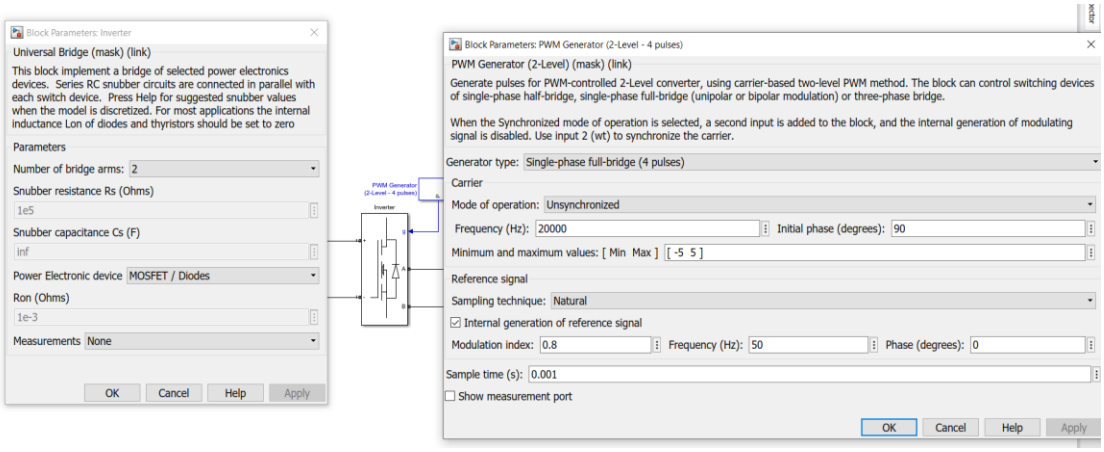

Fig. 4.13. Configuration of the implemented inverter

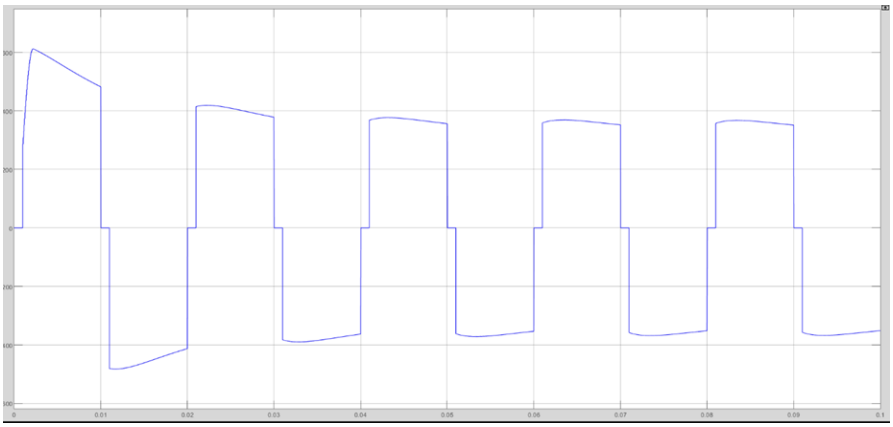

Fig. 4.14. The voltage at the output of the single-phase inverter

In order to bring the shape of the signal as close as possible to a sinusoidal signal, a passive low-pass filter of the L-C-L type was provided.

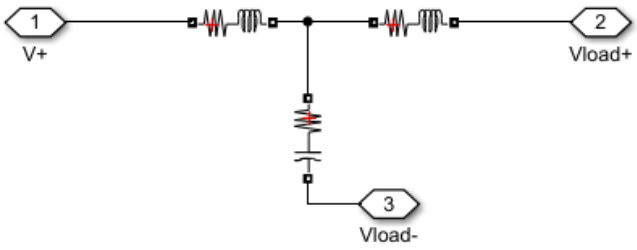

Fig. 4.16. L-C-L filter implemented

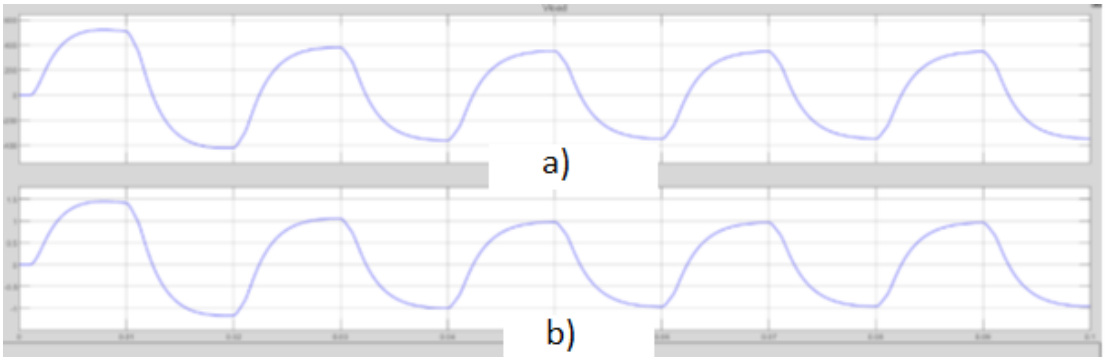

a) Output voltage
b) Output current intensity

Fig. 4.17. L-C-L filter operation

CHAPTER 5. Extending the Battery Bank Model to Incorporate different technologies

5.1. Extension of the model for a Pb-acid battery

The data needed to extend the model was obtained from a VRLA 12 V 9 Ah lead-acid battery, model FC12-9, used in stationary applications (UPS). This battery is similar to the ones used in the studied UPS in terms of performance, but it is produced by a different company. The parameters of the studied battery are presented in Table 5.1.

Nr. Crt.	***Parameter***	***Value***
1	Nominal voltage	12 V
2	Nominal capacity	9 Ah
3	Minimum admissible voltage (discharge)	10,50 V
4	Maximum permissible voltage (charge)	14,5 V
5	Maximum charging current	1,8 A
6	Nominal discharge current	0,45 A

Test assembly – Fig. 5.2 includes a programmable electronic load and the necessary command and recording software

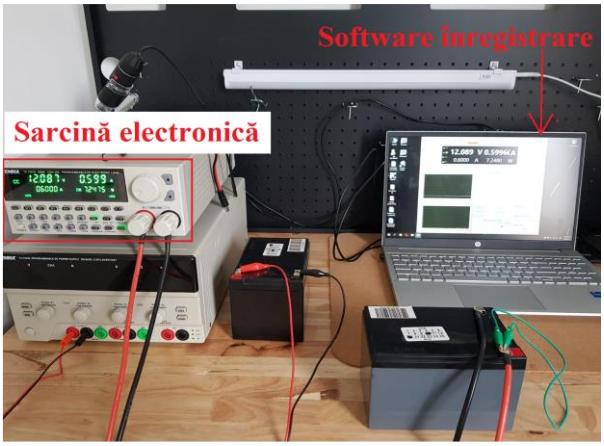

Fig. 5.2. Experimental assembly used to carry out the constant current discharge test

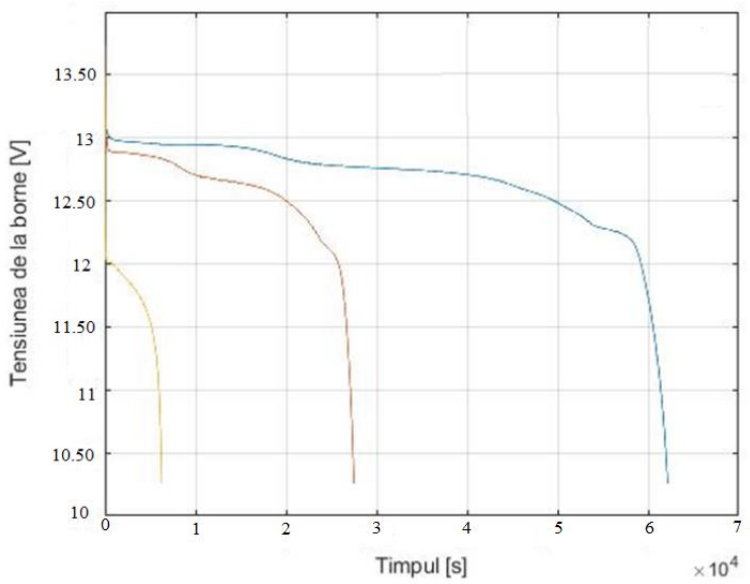

Fig. 5.3. Cycle 3 of the constant current discharge test sequence

The configuration of the battery pack is shown in Fig. 5.5. After running the simulation, the SoC evolution for 5 s is shown in Fig. 5.6. In this range the SoC drops from 100% to 99.86%, which means a discharge speed of 1.56%/min, from which it follows that a decrease in the nominal capacity from 100% to 80% will be made in 11'58".

5.2. Extension of the model for a Li-Ion battery

The Li-Ion battery considered to be used as a power source for the UPS is of the LiCoO2 type, produced by the SAMSUNG company and which has a rated discharge current close to that of the VRLA battery. The main operating parameters presented in Table 5.2.

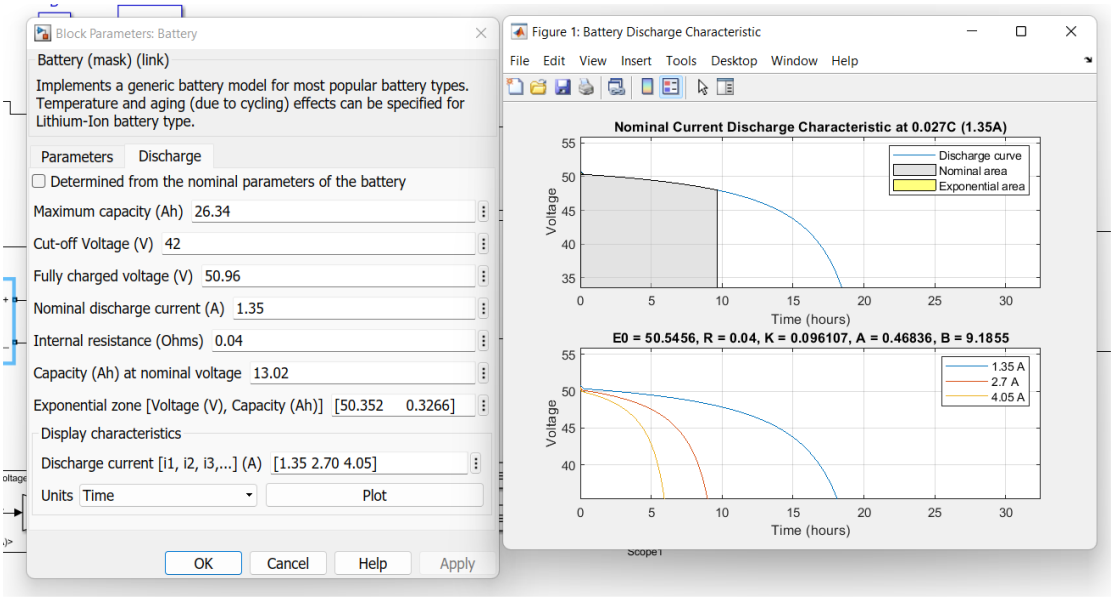

Fig. 5.5. VRLA battery configuration obtained from measured data

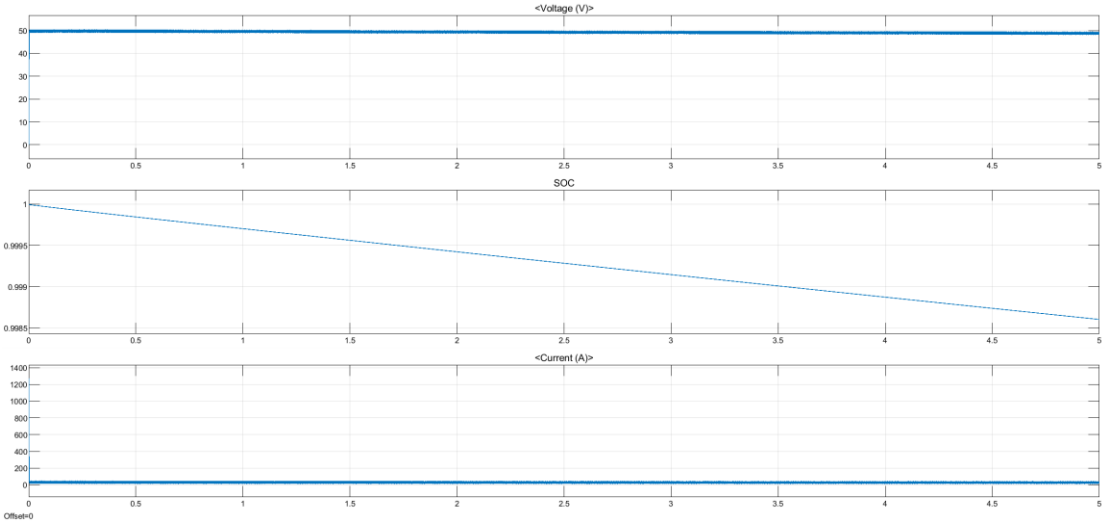

Fig. 5.6. SoC Evolution of 4S3P VRLA Battery Bank

Table 5.2. Li-Ion battery parameters

Nr. Crt.	***Parameter***	***Value***
1	Nominal voltage	3,6 V
2	Nominal capacity	2,5 Ah
3	Minimum admissible voltage (discharge)	2,5 V
4	Maximum permissible voltage (charge)	4,2 V
5	Maximum charging current	1,25 A
6	Nominal discharge current	0,5 A

The same unloading steps were followed according to the USABC methodology, the results obtained being shown in Fig. 5.7

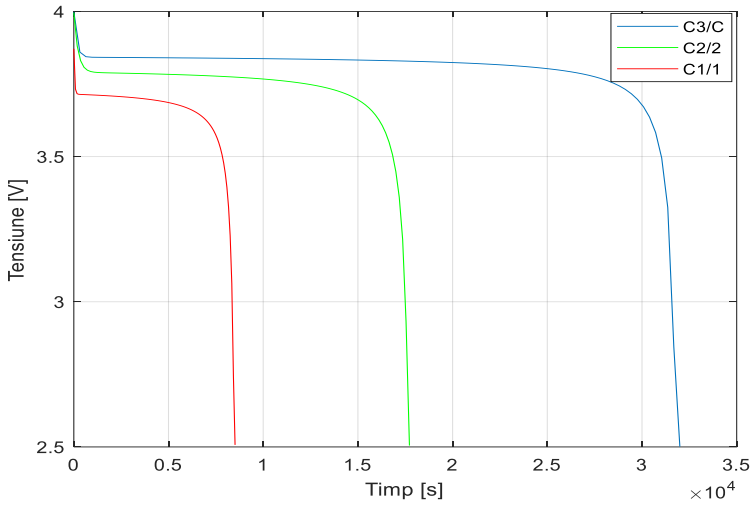

Fig. 5.7. Cycle 3 of the constant current discharge test sequence

The effective battery capacity was also calculated based on the arithmetic mean of the three C3/3 capacities, which is 2.47 Ah.

Next, a discharge test was performed using the nominal current I = 0.5 A and the rest of the parameters required for the model were extracted from the obtained curve - Fig. 5.8.

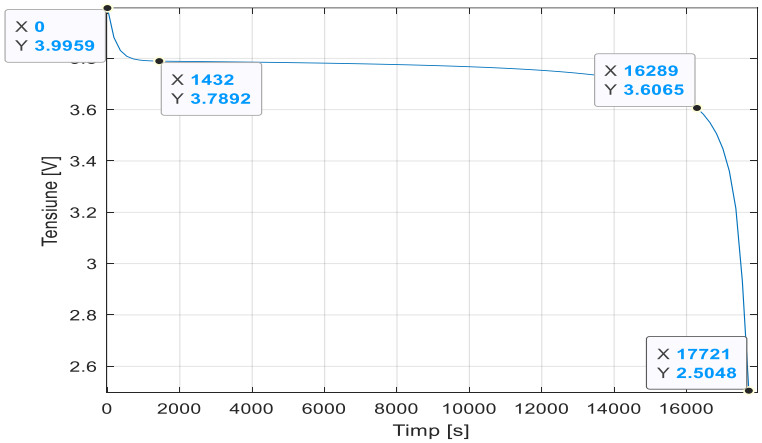

Fig. 5.8. Discharge at nominal current I = 0.5 A to determine the coordinates needed for the model

Considering that all batteries are identical, by extrapolation a configuration as close as possible to that of the VRLA battery was proposed, namely 13S11P. The configuration of the battery pack is shown in Fig. 5.9

After running the simulation, the SoC evolution for 5 s is shown in Fig.5.10.

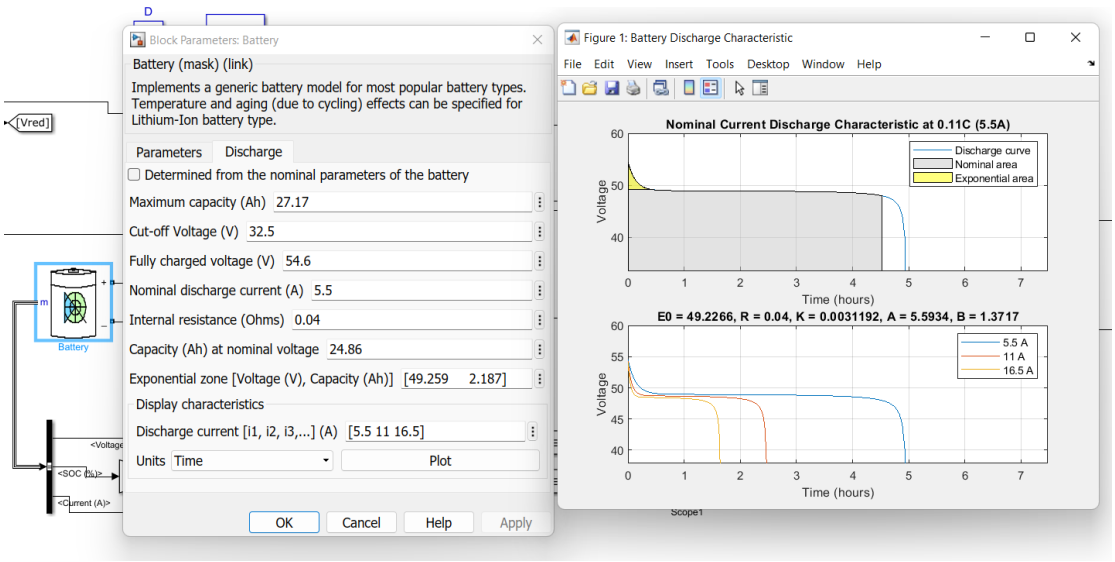

Fig. 5.9. Li-Ion battery configuration

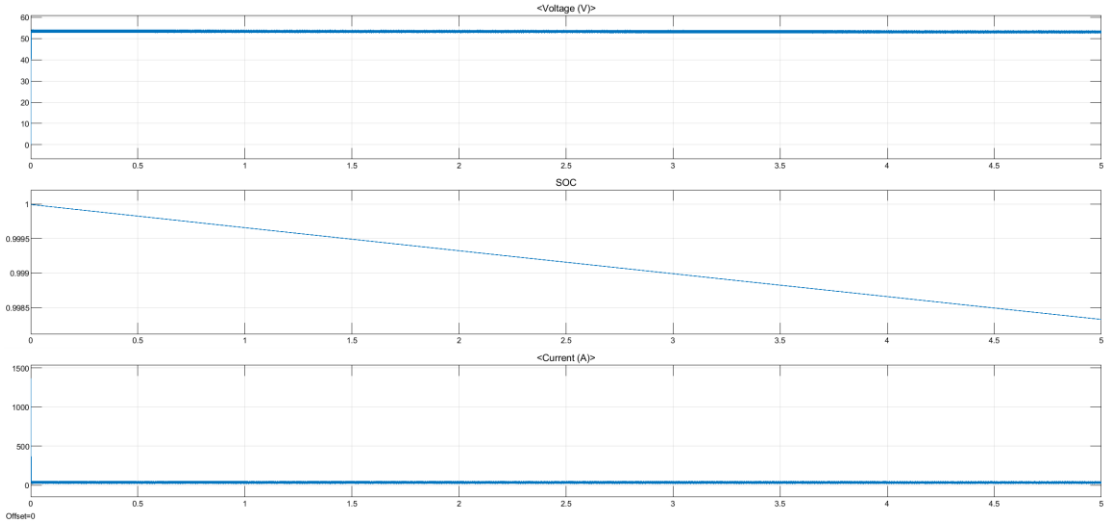

Fig. 5.10. SoC evolution of the 13S11P Li-Ion battery bank

In this range the SoC drops from 100% to 99.84%, which means a discharge speed of 1.92%/min, from which it follows that a drop in nominal capacity from 100% to 80% will be made in 10'50". This first capacity estimate is lower than the determined reference variant, which is why 2 more batteries will be inserted in the parallel configuration resulting in 13S13P. The new configuration of the Li-Ion battery bank is the one in the following figure.

For this new configuration, a variation of the SoC is obtained for a 5 s interval between 100% and 99.86% - Fig. 5.13, similar to that of the VRLA battery.

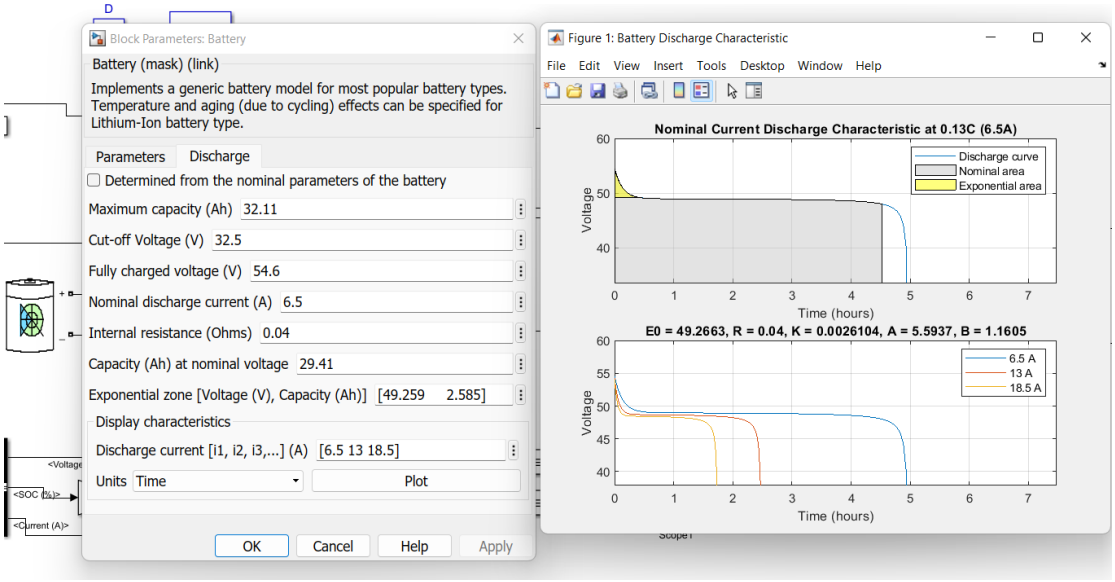

Fig. 5.11. The new Li-Ion configuration

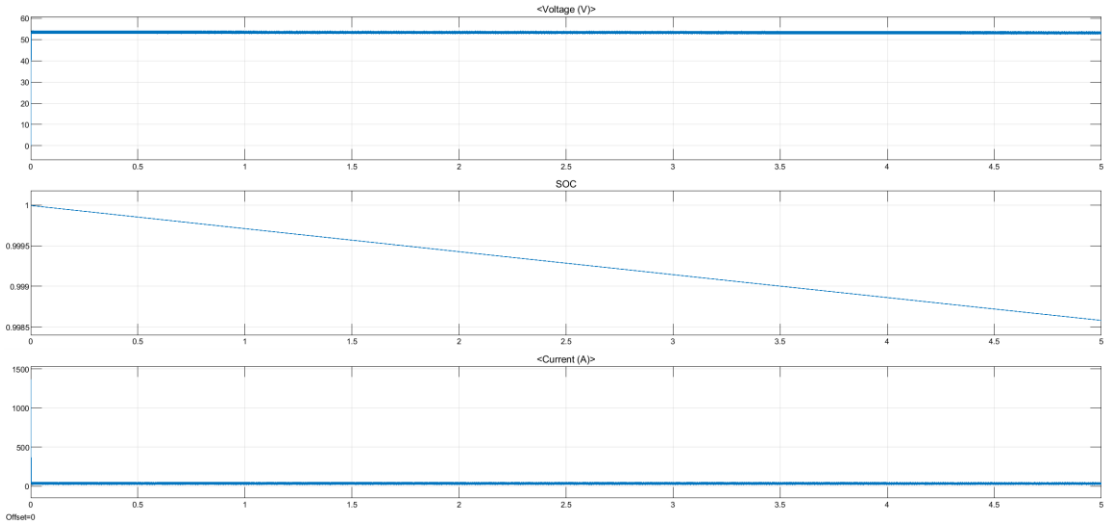

Fig. 5.12. SoC evolution of the 13S13P Li-Ion battery bank

The Li-Ion battery that was used in the study was a new one. This also implies a high cost price for equipping a UPS, but in the current context there is also another power supply solution for Li-Ion batteries, the so-called second-life batteries.

5.3. Extension of the model for a second-life LiFePO4 battery

To study the behavior of an online UPS equipped with second-life batteries, a new LiFePO4 cell that was artificially aged was started. For this, a cell produced by the HETER company was chosen which has the pre-aging parameters shown in Table 5.3.

Table 5.3. LiFePO4 battery parameters [94]

Nr. Crt.	Characteristic	Value	U.M.
1	Nominal capacity	1400	mAh
2	Rated discharge current	700	mA
3	Maximum charging current	2100	mA
4	Peak current (<1s)	5600	mA
5	Minimum admissible voltage	2.5	V
6	Maximum admissible voltage	3.6	V
7	Internal resistance	60	mΩ

Before aging the cell the USABC test sequence was applied and the effective capacity of 48 Ah was determined.

Aging of the cell was done using the test sequence known as Random Walk which involves the application of a sequence of charge and discharge currents, each lasting 5 min, starting from a fully charged battery. Test sequence – Fig. 5.13, it consists of 12 steps for an hour, respectively approximately 100 steps (96 steps) for a day (8 hours).

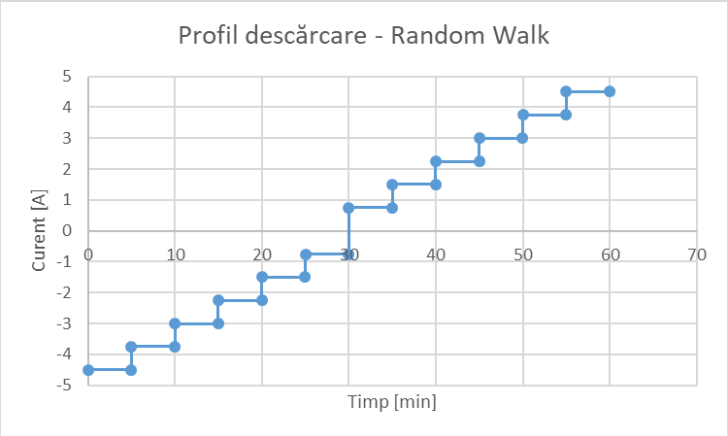

Fig. 5.13. Random Walk download profile

After applying 500 steps of the Random Walk sequence the USABC test method was applied again and the new effective cell capacity was 1.22 Ah, about 83% of the original capacity. Under these conditions, the state of health (SoH) of the cell is considered to be 83%. The following parameters will be considered for this aged cell - Table 5.4.

Table 5.4. Parameters of the second-life LiFePO4 battery

Nr. Crt.	Characteristic	Value	U.M.
1	Nominal capacity	1,220	Ah
2	Rated discharge current	0,610	A
3	Nominal voltage	3,2	V
4	Minimum admissible voltage	2,5	V
5	Maximum permissible voltage	3,6	V

Based on the discharge test at constant current I = 0.61 A, the discharge curve was obtained from which the rest of the parameters required for the model were extracted - Fig. 5.14.

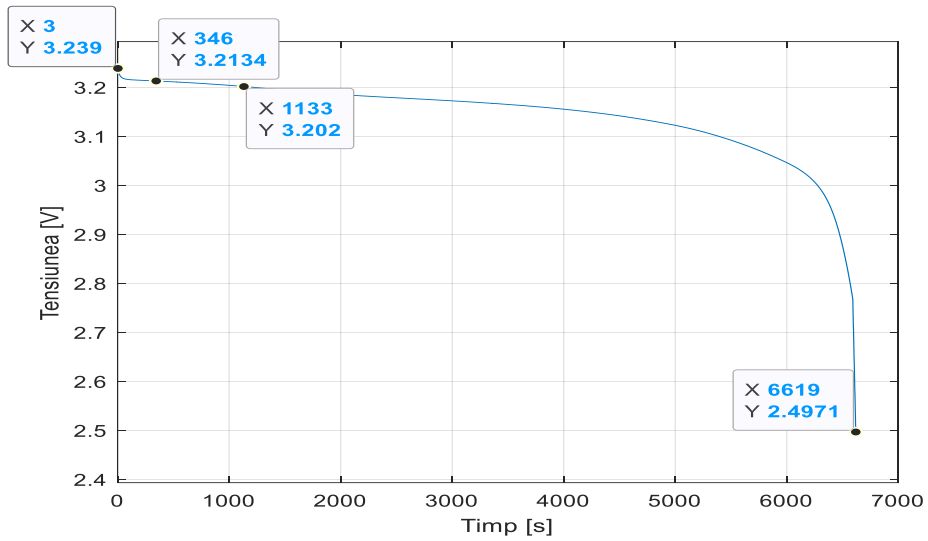

Fig.5.14. Discharge at nominal current I = 0.61 A for determining the required model coordinates

Assuming that all batteries are identical, by extrapolation a configuration as close as possible to that of the VRLA battery was proposed, i.e. 15S22P The configuration of the battery pack is shown in Fig. 5.15.

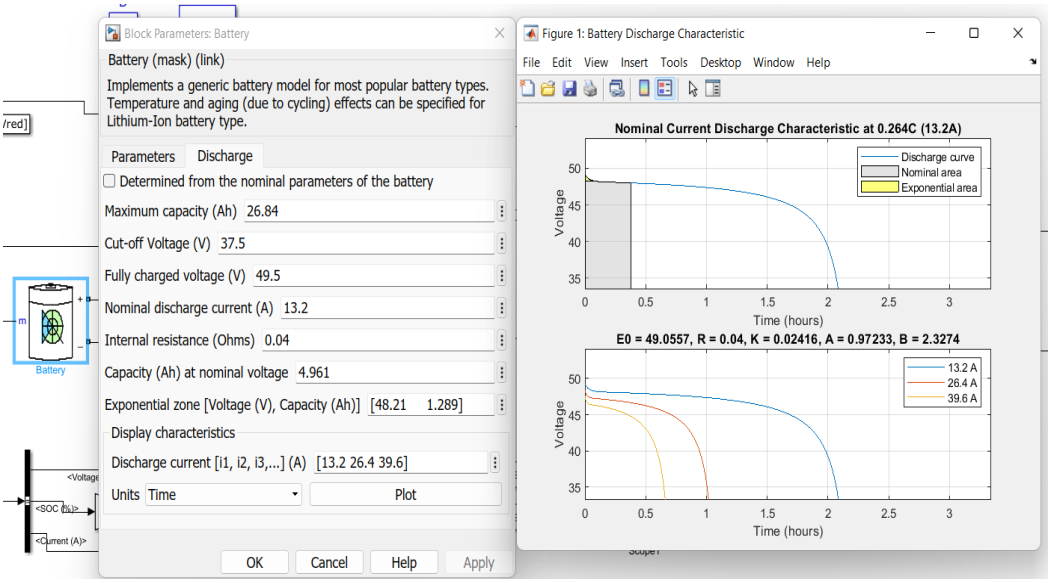

Fig.5.15. LiFePO4 cell configuration

After running the simulation, the SoC evolution for 5 s is shown in Fig. 5.16.

In this interval the SoC decreases from 100% to 99.87%, which means a discharge rate of 1.56%/min, from which it follows that a decrease of the nominal capitation from 100% to 80% will be done in 12'04".

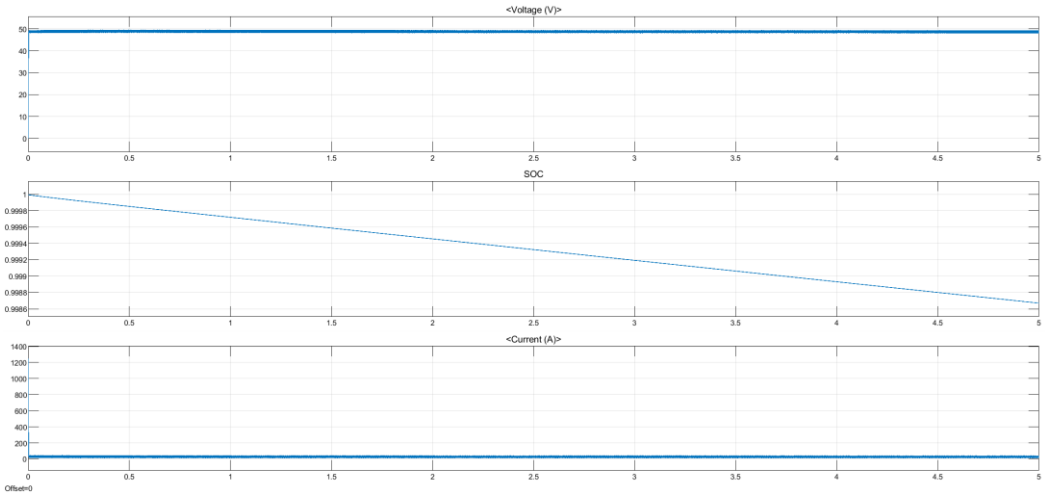

Fig.5.16. SoC evolution of the 15S22P LiFePO4 battery bank

This first capacity estimate is higher than the determined reference variant, which is why one cell will be extracted from the resulting parallel configuration 15S21P. The new Li-Ion battery bank configuration is:

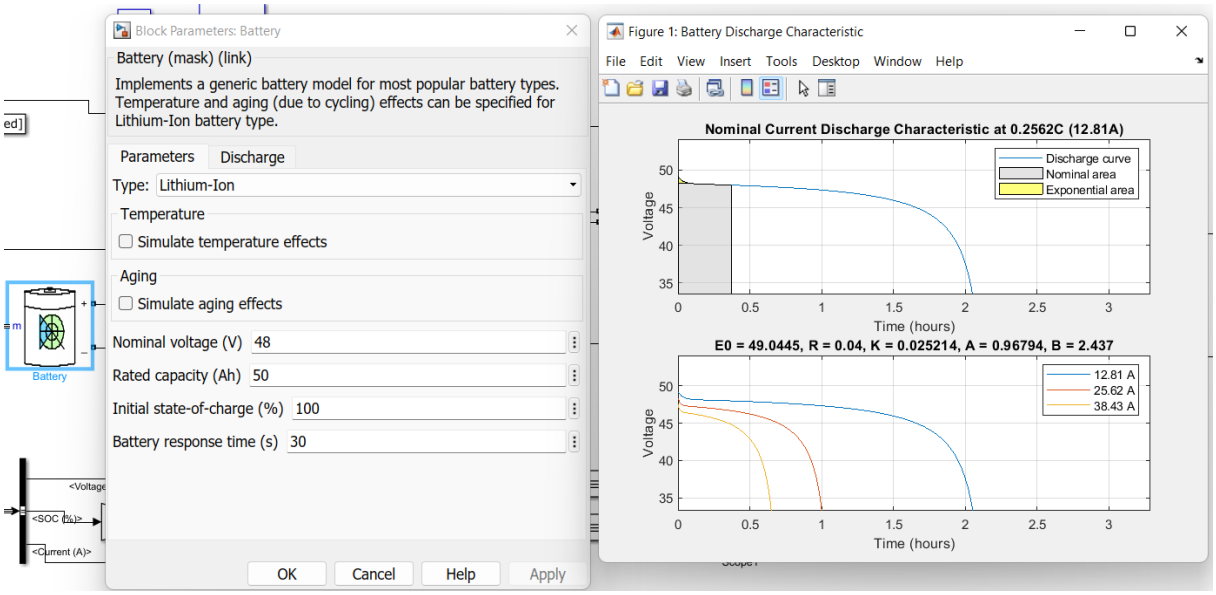

Fig.5.17. New LiFePO4 cell configuration

For this new configuration a variation of the SoC for a 5 s interval between 100% and 99.86% is obtained - Fig. 5.18, similar to that of the VRLA battery.

The LiFePO4 battery is characterized by a high current density, which leads to a lower number of batteries than theoretical even under reuse conditions.

The results demonstrate that there are viable alternatives to Pb-acid batteries equipping UPS in Data Centres.

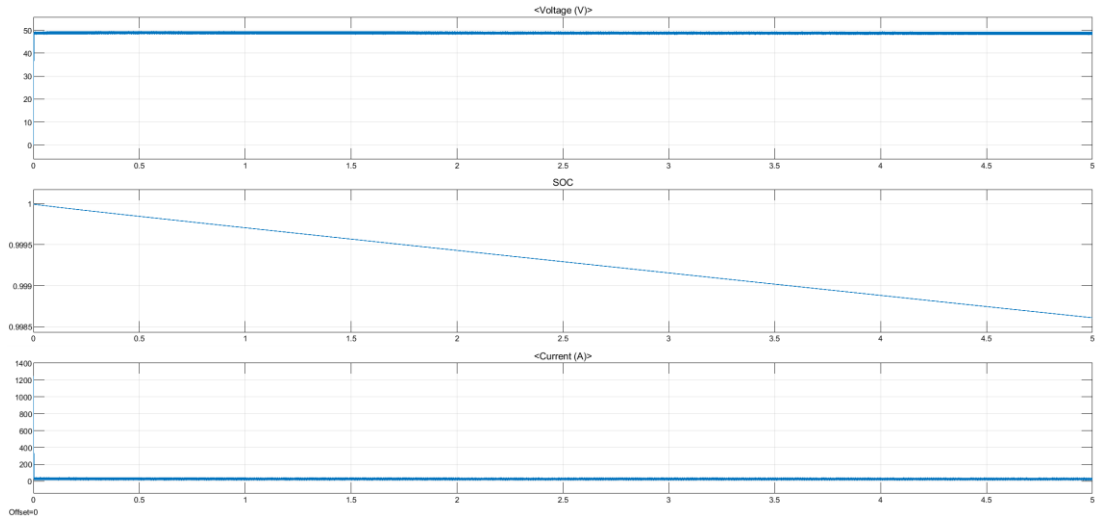

Fig. 5.18. SoC evolution of the 15S21P LiFePO4 battery bank

Chapter 6. Design and implementation of a system to determine the health of a Pb-acid battery equipping a UPS

Determining the optimal time for replacement can be thought of in economic terms, but always based on an estimate of the age of the battery. This process is quantified by the State of Health (SoH) and depends on the nominal capacity of the battery and the actual capacity at a given point in time. Because the UPS must ensure uninterrupted power operation, a battery is considered to have reached its life limit when the SoH value falls below 80% [38].

Based on these assumptions, the specifications to be met by the proposed battery age determination system were formulated:

- System minimally invasive that does not disturb the UPS operation;
- Independent of historical information on battery evolution;
- Battery age with a relative error below 5%;
- System with low complexity and small footprint.

6.1. Two-pulse discharge method

The application of the discharge method is done according to the following methodology:

1.Disconnect the battery from the load/charging system for at least 2 minutes

2.After this period, the voltage at the battery terminals shall be considered as open circuit voltage OCV

3.Apply the test sequence in Fig. 6.1

4.Measure the value of the voltage drop ΔV2 after the second discharge pulse

5.Predict the nominal discharge current coefficient Cr according to the relationship

$C_r = \delta \cdot (\Delta V_2) + \gamma$,

where are obtained from Fig. 6.2.

6.Calculate the state of charge of the battery with the relation

$SoC = \frac{V_{max} + \beta - EMF_{min}}{\alpha}$,

where Vmax, EMFmin, and is determined from the discharge data provided by the battery manufacturer.

7.Predict the maximum effective capacity remaining in the battery based on the equation

$C_{ef} = \frac{1}{C_r}$

8.Determine the health of the battery from the relationship

$SoH = \frac{C_{ef}}{C}$,

where C is the rated capacity of the battery according to the battery manufacturer's data.

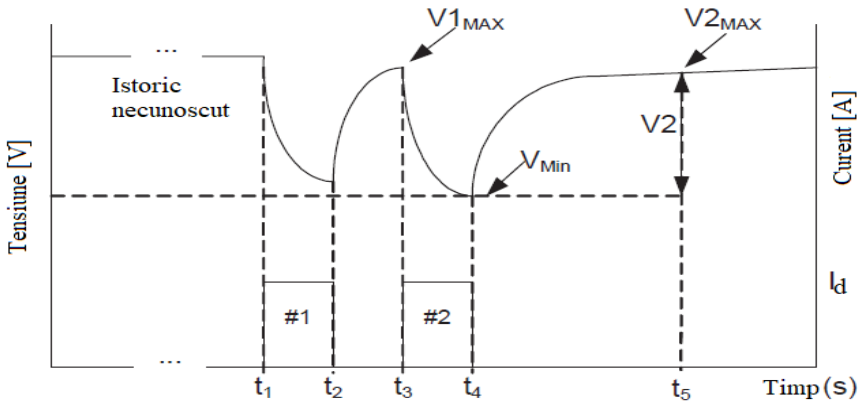

Fig. 6.1. Test sequence for the two-pulse method [94]

Table 6.2. Dependence of the nominal discharge current coefficient and discharge current [95]

Nr. Crt.	Discharge current [A]	Expected discharge current coefficient Cr
1	10	1,093
2	25	2,732
3	35	3,825
4	50	5,464
5	65	7,104
6	80	8,743

6.2. Hardware structure of the proposed system

The wiring diagram of the developed prototype is shown in Fig. 6.3.

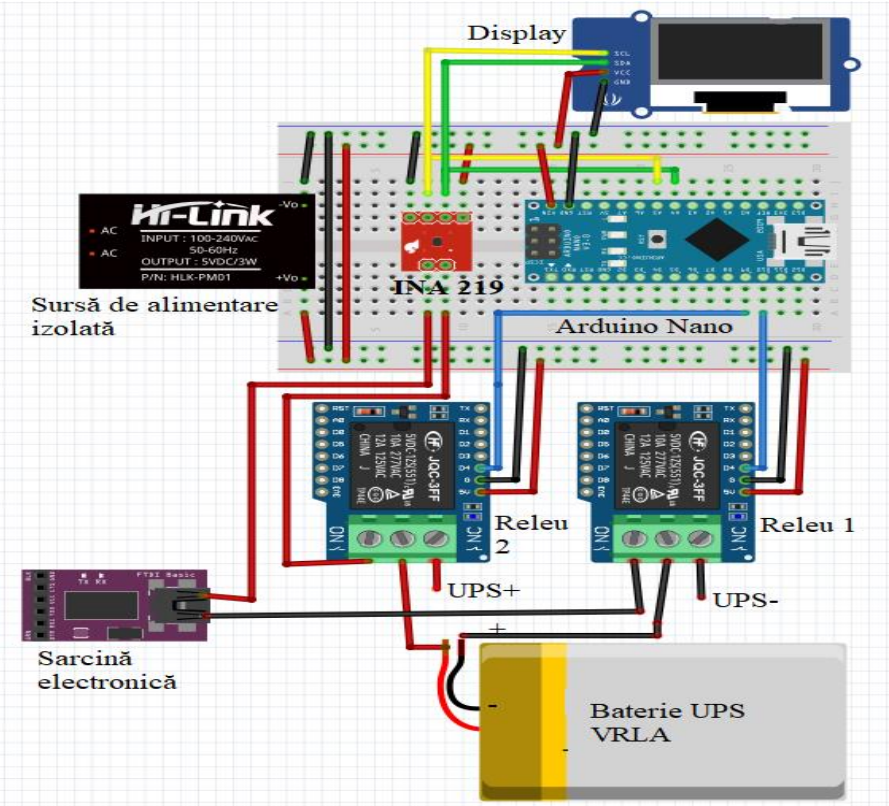

Fig. 6.3. Wiring diagram of the developed prototype

The central element of the scheme is the electronic load that applies to the VRLA battery the two current pulses necessary to obtain the voltages ΔV2 and Vmax. The coupling of the electronic load is done through the normally open (ND) contacts of the two relays. The control sequence is provided by the Arduino Nano unit which, based on current and voltage information from the INA219 integrated sensor, determines when the test sequence can be applied. This sequence consists of applying two 1A current pulses for 18 seconds and recording the voltages at the beginning and end of each pulse.

The scheme is completed by the isolated power supply which connects to the mains and provides a DC voltage of 5 V for the operation of the prototype while providing galvanic isolation.

Data on recorded and estimated magnitudes, SoC and SoH are displayed on a colour OLED screen.

The electronic load used was developed for testing USB ports and is composed of an IRFZ44 MOSFET with a working range between 3.7V and 13 V. It is controlled by an LM324 operational amplifier with a potentiometer on the inverting input that allows the current to be adjusted in the range 0.15 A...3 A. The load is complemented by a temperature measurement circuit on the MOSFET and an active cooling system that intervenes when the power dissipation reaches the threshold value of 13 W. To keep the load operating within these limits, the discharge current was set at 1A for all tests.

The measurement circuit is based on the INA 219 integrated circuit which allows the simultaneous measurement of voltage in the range 0 ... 26 VDC and current in the range 0... 3.2 A. For this purpose, an operational amplifier in differential configuration is used which measures the voltage drop across a shunt resistor with a value of 10 Ω. The measured voltages are converted by a 16-bit DAC and transmitted over the I2C interface to the control system.

The controller is from the Arduino (Nano) family and is based on an Atmega328 processor with AVR architecture providing 16 MHz processing frequency and 32 kB program memory. It also has I2C, SPI, serial and USB communication interfaces. Data is displayed on a 128x64 px colour OLED technology screen with a diagonal of 0.96". Brightness and very high contrast are adjustable via the built-in controller and communication is via the SPI interface. Power consumption is a very low 0.08 W.

6.3. Software structure of the proposed system

The software structure was developed in accordance with the test methodology and the developed hardware structure. The source code flowchart is shown in Fig. 6.4.

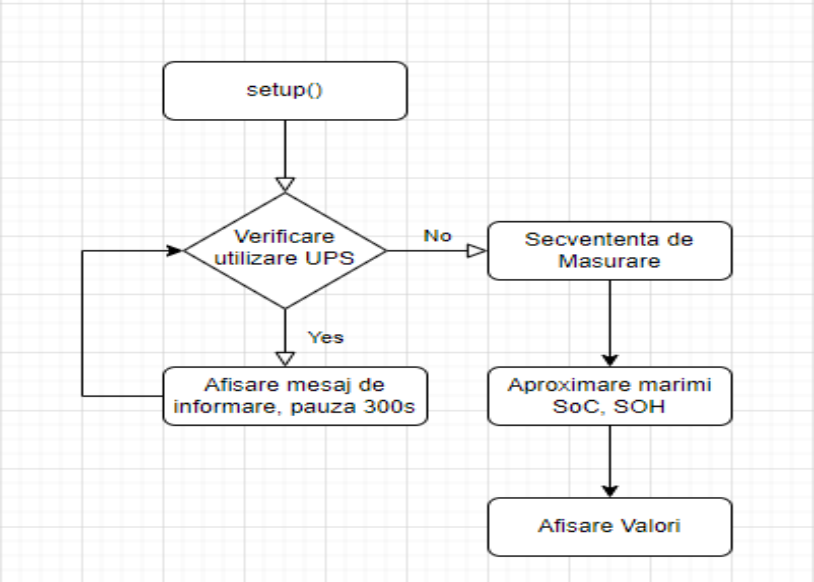

Fig. 6.4. Source code flowchart

In addition to the developed functions, a number of libraries were used to communicate with the hardware elements of the scheme:

□<Wire.h> - the I2C communication library used by the INA219 integrated sensor

□<Adafruit_INA219.h> - library for processing information from the INA219 sensor

□<SPI.h> - SPI communication library used by the OLED display

□<Adafruit_GFX.h> - library used for displaying messages on the screen

□<Adafruit_SSD1306.h> - library used as device driver

The code sequence used by the setup() function is used to initialize communication with peripheral systems and set the input and output pins used.

The source code developed for this function is presented in the thesis:

6.4 Calibration of the developed SoC and SoH determination system

The calibration of the SoC and SoH determination system was done using the test structure in Fig. 6.5 and the experimental data obtained. The chosen structure uses instead of a VRLA battery a programmable voltage source that can reproduce, over the duration of two 18 second pulses, the voltage drop across the terminals of a battery under test.

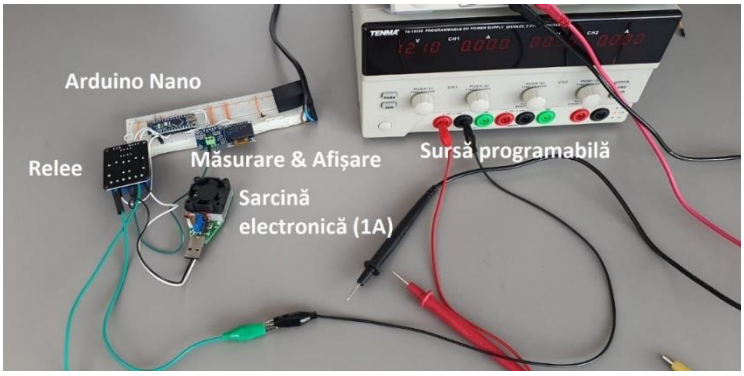

Fig. 6.5. Structure used for calibration

The experimental data used are shown in Fig. 6.6 and represent the voltage variation ΔV2 as a function of Crate. Since in the tests performed in [81] a discharge current of 10 A was used, which cannot be reached by the developed system, based on the data in Table 6.2 the value for Crate corresponding to a discharge current of 1A was extrapolated, obtaining Crate = 0.1093 Ah.

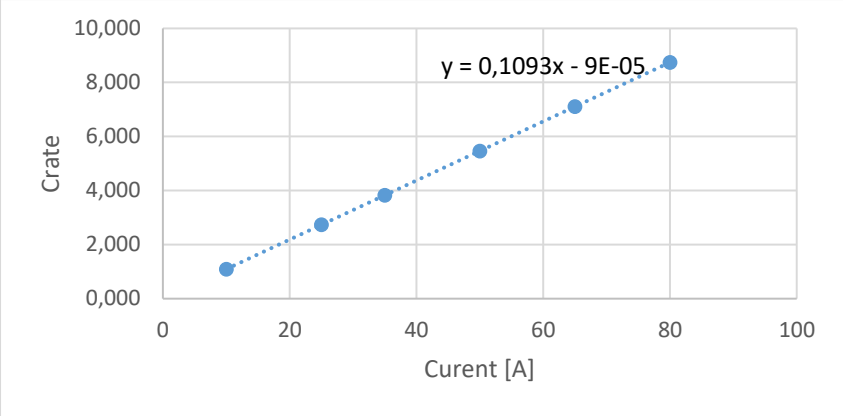

Fig. 6.6. Crate evolution as a function of discharge current - representation of the data in Table 6.2.

For a variation ΔV2 = 0.07 V, the VRLA battery tested in [83] had a nominal capacity of 183 Ah, and a SoC = 80%, respectively SoH = 80%. The experimentally obtained values fall within a maximum relative error of 2% for SoC, respectively 0.5% for SoH. They validate the extrapolated value for Crate and make the system ready for VRLA battery testing.

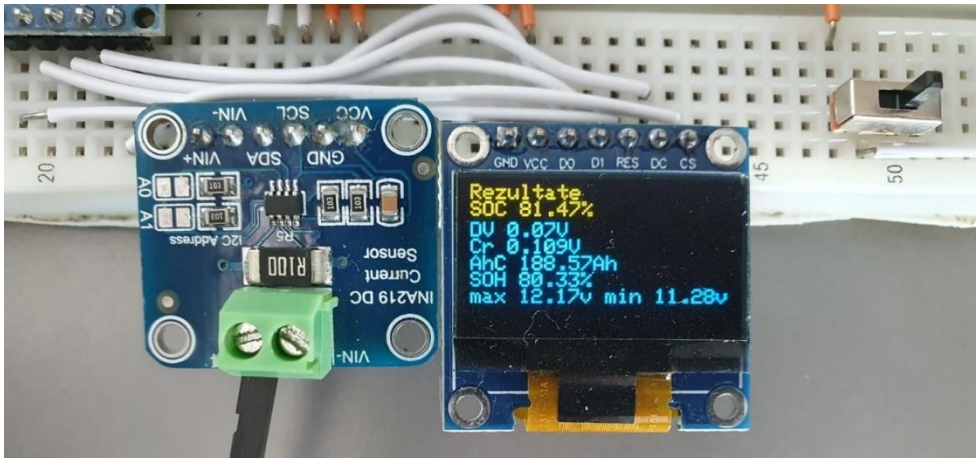

Fig. 6.7. System calibration results

6.5. Experimental results of SoC and SoH determination of batteries equipping UPSs

The final form of the developed prototype is shown in Fig. 6.8. It follows the scheme developed during the design process and includes all the source code presented.

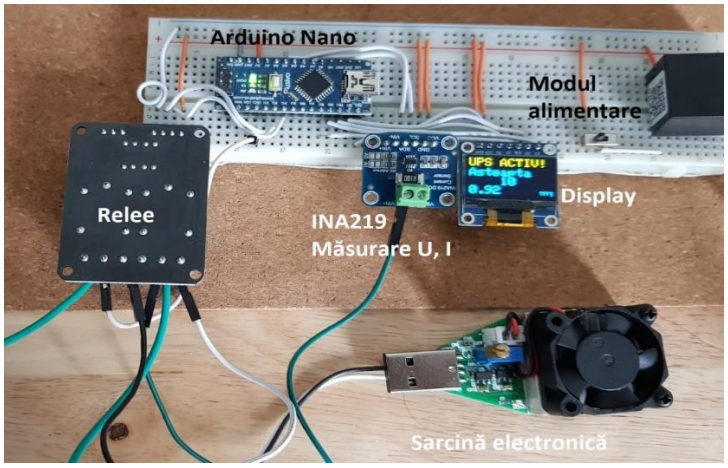

Fig. 6.8. Developed prototype

The data of the three batteries are summarized in Table 6.3.

Table 6.3. Status of batteries under test

Nr. Crt.	Rated capacity [Ah]	Health status *SoH* [%]
1	9	92
2	12	86
3	14	81

The following values were obtained for the three batteries:

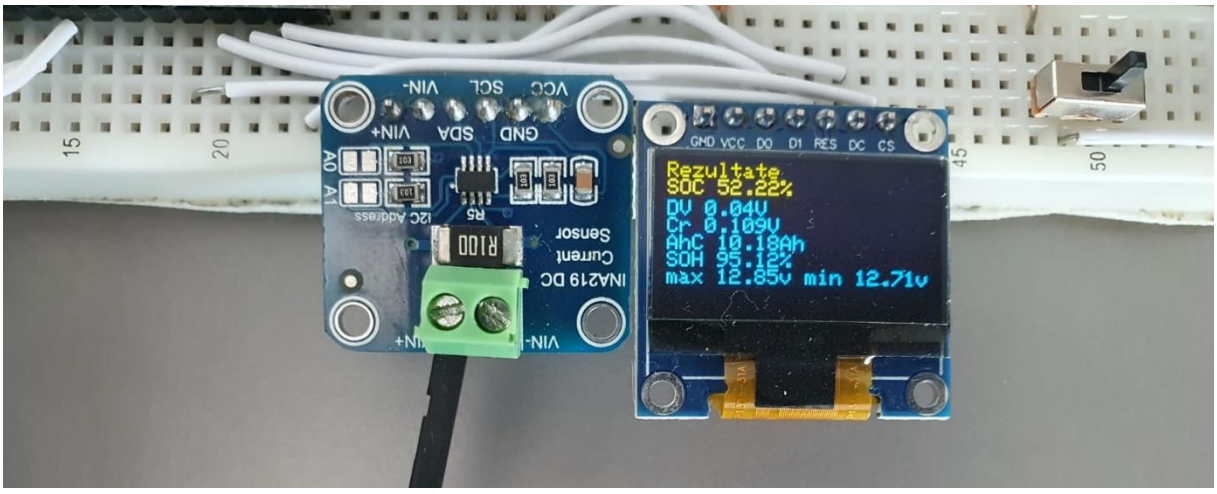

a) Battery 1 - 9Ah, SoC = 60%, SoH = 92%.

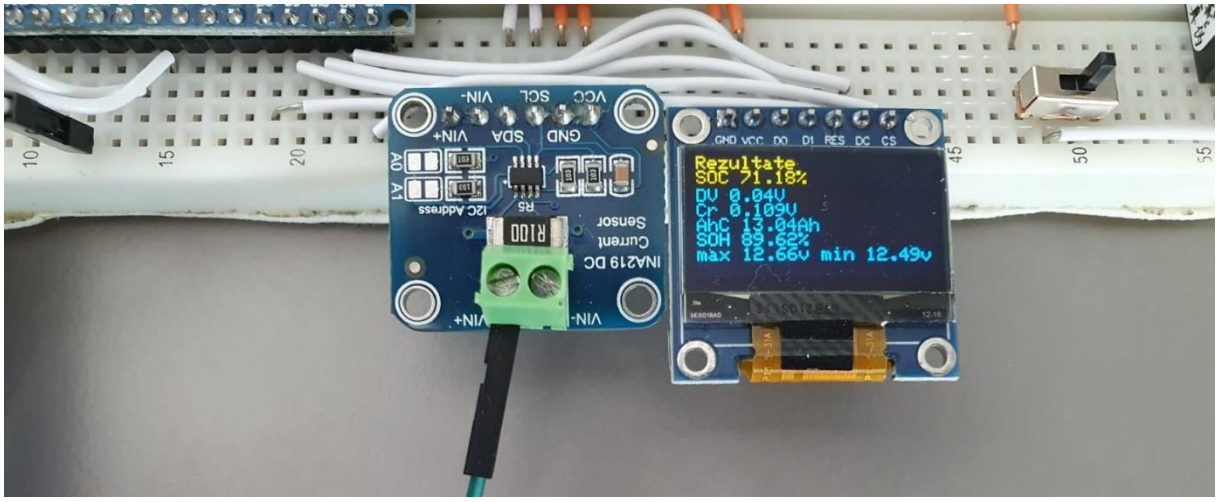

b) Battery 2 - 12Ah, SoC = 75%, SoH = 86%.

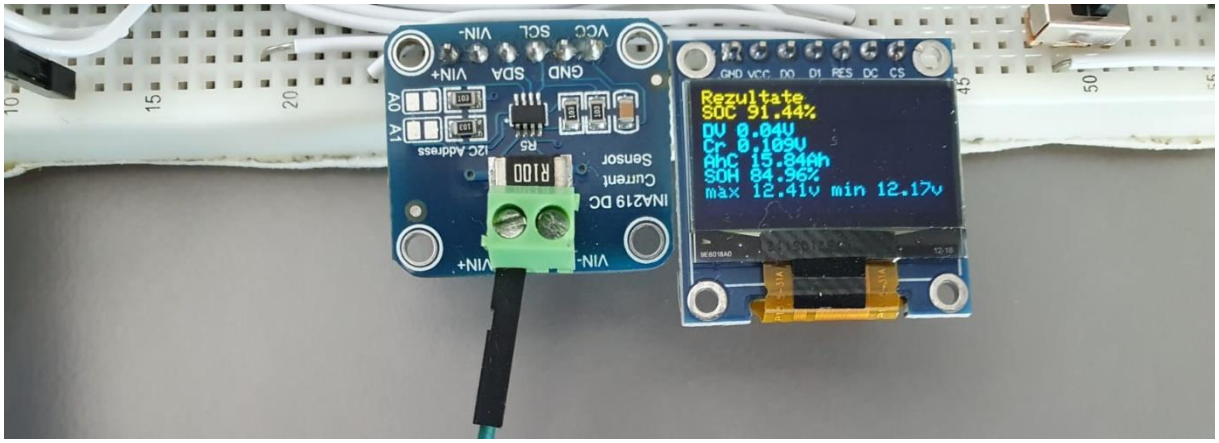

c) Battery 3 - 14Ah, SoC = 90%, SoH = 81%.

Fig. 6.9. Experimental results obtained from testing the three VRLA batteries

The absolute errors and relative errors for SoC and SoH determination are shown in Table 6.4.

Table 6.4. Evaluation of the accuracy of the SoC and SOH estimation system

Nr. Crt.	*SoC* real [%]	Estimated SoC[%]	Absolute error [%]	Relative error [%]	Actual SoH	[%] Estimated SoH [%]	Absolute error [%]	Relative error [%]
1	60	52,22	7,78	**12,96**	92	95,12	-3,12	3,39
2	75	71,18	3,82	5,09	86	89,62	-3,62	4,20
3	90	91,44	-1,44	1,60	81	84,96	-3,96	**4,88**

The relative errors obtained in the SoC estimation are in the range of 1.60 - 12.96 %, exceeding the limit of 5 % which is considered the standard in the field, only for battery No.1. It should be noted that the SoC estimation method based on two discharge pulses is used only in the range of 40 - 100

%, which makes the SoC of battery No.1 fall in the first third of the measurement range where errors with values higher than 10 % are accepted.

For SoH estimation the error range is much narrower 3.39 - 4.88 %, below the 5 % limit, the maximum error being obtained for the SoH with the lowest value. Also, VRLA batteries used in UPSs are considered to have reached their lifetime around 80% SoH (which is why these batteries were chosen for the study), allowing a measurement limit of 83% to be imposed in the use of the device, below which VRLA batteries need to be replaced. This limit was chosen because the estimated SoH from the measurements made is generally higher than the real SoH.

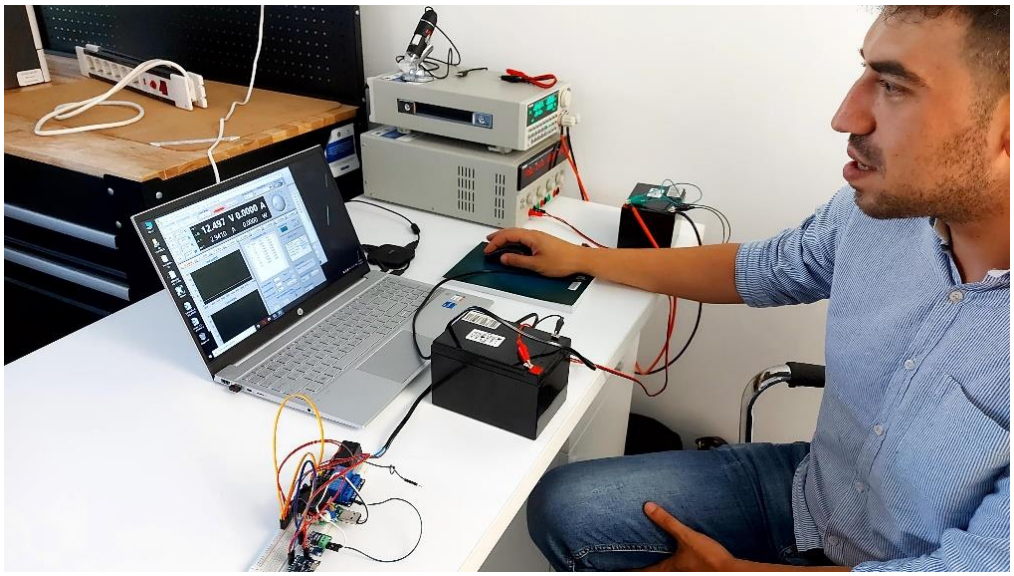

CONCLUSIONS

General conclusions

This paper addresses the complex issue of uninterruptible power supply systems for sensitive electrical equipment connected to the grid.

Backup systems (UPS) are currently at a technological crossroads, with old VRLA batteries about to be replaced by Li-Ion batteries. However, most UPSs today still use VRLA batteries and are not equipped with health monitoring systems (SoH).

In this context, the present paper is an answer to these two major problems. By building a functional model of a UPS, it is possible to accurately determine the parameters of a Li-Ion battery that can replace a VRLA battery, and the developed prototype also ensures a highly accurate estimation of the health status of VRLA batteries in operation in UPSs without advanced management systems.

Based on the study of UPS topologies that are used in Data Centres and other power-sensitive locations, based on the information obtained from an operational UPS, a functional block-level model of an online UPS was developed. This model has been validated with experimental data allowing the study of different battery technologies as a backup power source for a UPS. The developed model

represents an optimized alternative to the classical method based on apparent consumer power alone when determining battery bank capacity.

With the developed prototype, the health status of VRLA batteries can be accurately estimated, thus bringing a new level of optimization to their use. Thus, the time at which a VRLA battery needs to be replaced is accurately determined, even if the UPS is not equipped with a management system to monitor this.

Personal contributions

In view of the above, I can state that the personal contributions in the present PhD thesis have taken into account the following directions:

- Conceptual: studying the main realization technologies for UPS and the batteries that equip them;

- Experimental: development of a prototype for testing VRLA batteries in order to estimate SoC and SoH, respectively, a prototype validated experimentally;

- Tehnologic: development of a methodology to determine the capacity of a Li-Ion battery that can replace a VRLA battery in a UPS, based on a functional UPS model and battery operating data provided by the manufacturer.

I appreciate your personal contributions to the field:

1.An extensive study, based on a large number of bibliographical references, on the current technologies for UPSs and the batteries that equip them.

2.A comprehensive literature study on battery modelling to integrate the battery model into the functional model of the UPS.

3.Development of a functional model for an experimentally validated UPS-online

4.Development of a new methodology to determine the optimal capacity of a VRLA, Li-Ion or LiFePO4 second-life battery that can equip a UPS, based on the developed model.

5.Study of the main methods for examining the state of charge and health of a VRLA battery

6.Design and realization of an equipment used to determine the SoC and SoH of a VRLA battery equipping a UPS.

7.Development of a new replacement methodology for VRLA batteries based on the prototype.

Selective bibliography

[1] *** ANSI/TIA-942 Standard , www.tiaonline.org/standards

[2] Chafai, S, TIA-942 Data Centre Standards Overview, https://www.academia.edu/14509572/

[3] *** EN 50600 Data Center Standards, https://www.tuvit.de/en/services/data-centers-colocation-cloud-infrastructures/din-en-50600/

[4] *** Data Center 2025: Exploring the Possibilities, EmersonNetworkPower.com

[7] Hintemann, R. , Consolidation, Colocation, Virtualization, and Cloud Computing – The Impact of the Changing Structure of Data Centers on Total Electricity Demand. Advances in Intelligent Systems and Computing, Springer Berlin Heidelberg.

[8].Harkeeret, S., The Green Grid's Data Center Maturity Model, www.thegreengrid.org

[9] Liam Newcombe, Data centre energy efficiency metrics, https://dcgs.bcs.org

[12] *** http://www.google.co.in/green/bigpicture/#/

[13]*** http://www.datacenterknowledge.com/archives/2015/04/27/second-yahoo-data-center-comes-online-in – new-york-state

[14] *** http://technet.microsoft.com/en- us/library/cc700692.aspx

[16] *** https://datacentercatalog.com/romania

[17] *** https://datacentercatalog.com/greece

[18] *** Data Center Infrastructure Resource Guide, ANIXTER, www. anixter.com

[19] Wendy, T, Types of Prefabricated Modular Data Centers, White Paper 165, Schneider Electric

[22] *** Optimal Solutions for Data Center Connect (DCC), Strategic White Paper, www.alcatel-lucent.com

[24] *** AC vs. DC in a battle for data center efficiency, www.itworld.com/data-centerservers/.

[26] Hallahan, R, Data center design decision and their impact on power system infrastructure, White Paper, www.cumminspower.com

[28] *** The large UPS battery handbook, Eaton.com/UPSbatteries

[32] Wu, H., Data Center Energy, White Paper 01- Development of the UPS Architecture, https://e.huawei.com/en/material/networkenergy/dcenergy

[34] G. J. May, A. Davidson and B. Monahov, Lead batteries for utility energy storage: A review, J. Energy Storage, 2018, 15, 145–157.

[38] S. Bobba, F. Mathieux, and G. A. Blengini, How will second-use of batteries affect stocks and flows in the EU? A model for traction Li-ion batteries, Resour. Conserv. Recycl., vol. 145, no. October 2018, pp. 279–291, 2019.

[39] M. S. H. Lipu et al., A review of state of health and remaining useful life estimation methods for lithium-ion battery in electric vehicles: Challenges and recommendations," J. Clean. Prod., vol. 205, pp. 115–133, 2018.

[40] L. C. Casals, B. A. García, F. Aguesse and A. Iturrondobeitia, Second life of electric vehicle batteries: relation between materials degradation and environmental impact, Int. J. Life Cycle Assess., 2017, 22, 82–93.

[44] J. Tian, R. Xiong, and W. Shen, A review on state of health estimation for lithium

ion, eTransportation, p. 100028, 2019.
[45] X. Lai, D. Qiao, Y. Zheng, M. Ouyang, X. Han, and L. Zhou, A rapid screening and regrouping approach based on neural networks for large-scale retired lithium-ion cells in second-use applications," J. Clean. Prod., vol. 213, pp. 776, 2019.
[46] ***USABC *Electric Vehicle Battery Test Procedures Manual*, http://www.uscar.org
[47] *** PNGV *Battery Test Manual*, Revision 3, 2001,
[52] Hu, M.,Li, Y., Li, S., Fu, C., Qin, D., Li, Z., Lithium-ion battery modeling and parameter identification based on fractional theory, Energy, 2018, 165, 153–163
[53] Doerffel,D., Abu Sharkh,S., A critical review of using the Peukert equation for determining the remaining capacity of lead-acid and lithium-ion batteries, Journal of Power Sources , (2006), 395–400
[55] Enache,B., Lefter,E., Stoica, C., Comparative Study for Generic Battery Models for Electric Vehicles, IEEE Xplore, ISBN 978-1-4673-5979-5, 2013
[56] Saxena, S., Raman, S.R., Saritha, B., John, V. A novel approach for electrical circuit modeling of Li-ion battery for predicting the steady-state and dynamic I–V characteristics. Sadhana, 2016, 41, 479–487.
[57] Sangwan, V., Sharma, A., Kumar, R., Rathore, A.K., Equivalent circuit model parameters estimation of li-ion battery: C-rate, soc and temperature effects. Proceedings of the 2016 IEEE International Conference on Power Electronics, Drives and Energy Systems (PEDES), Kerala, India, 2016, p 1-6
[58] Abbas, F., Auger,D., Propp, K., A review on electrtic vehicle battery modelling; From Lithium-ion toward Lithium -Sulphur, Renewable and Sustainable Energy Reviews, Vol.56, 2016, Pages 1008-1021
[60] Glass, M.C., Battery electrochemical nonlinear/dynamic SPICE model. Proceedings of the IECEC 96, Washington, DC, USA, 1996; Volume 1, pp. 292–297
[62] Pop,V, Bergveld,H. J., Notten, P. H., Op het Veld, L J. H. G and Regtien, P. P. L., Accuracy analysis of the state-of-charge and remaining run-time determination for lithium-ion batteries, Measurement, vol. 42, no. 8, pp. 1131–1138, 2009.
[63] Schweiger H-G, Obeidi O., Komesker, O., Comparison of Several Methods for Determining the Internal Resistance of Lithium Ion Cells, Sensors 2010,10, p.5604
[70] Zhao,G, Examples for Reuse of Power Batteries, In book: Reuse and Recycling of Lithium-Ion Power Batteries, May 2017, DOI: 10.1002/9781119321866.ch3
[71] Tang,I, and co., Predictive Maintenance of VRLA Batteries in UPS towards Reliable Data Centers, IFAC World Congress 2020
[72] Karpati,A, Zsigmond,G and co., UPS for data center, Intelligent Systems and Informatics (SISY), 2012 IEEE 10th Jubilee International Symposium
[73] Haider, A, Zhao,Q., Cluster-Based Prediction for Batteries in Data Centers, Energies 13(5):1085, 2020
[78] Glass, M.C., Battery electrochemical nonlinear/dynamic SPICE model. Proceedings of the IECEC 96, Washington, DC, USA, 1996; Volume 1, pp. 292–297
[79] *** Matlab, Generic Battery Model, https://www.mathworks.com/help/sps/powersys/ref/battery.html